Wrocław University of Science and Technology

Technology Arts Sciences TH Köln

MCG

Machine Control & Guidance

8th International Conference on Machine Control & Guidance

ONLINE | 17th – 18th November 2022

Proceedings

ISTVS LORMVE

Laboratory of Off-Road Machine and Vehicle Engineering

8th International Conference on Machine Control & Guidance

Proceedings

Online, 17th–18th November 2022

Oficyna Wydawnicza Politechniki Wrocławskiej
Wrocław 2022

Editorial Layout

Robert CZABANOWSKI

Technical Layout

Stanisław GANCARZ

Wrocław University of Science and Technology Publishing House
Wybrzeże Wyspiańskiego 27, 50-370 Wrocław
http://www.oficyna.pwr.edu.pl
e-mail: oficwyd@pwr.edu.pl
zamawianie.ksiazek@pwr.edu.pl

ISBN 978-83-7493-234-9
https://doi.org/10.37190/MCG2022

Contents

Agri-Food Competition for Robot Evaluation (ACRE), the design of a competition of the METRICS project

Daniel Boffety[1], Manon Boulet[1], Michel Berducat[1], Matteo Matteucci[2], Riccardo Bertoglio[2], Giulio Fontana[2], and Davide Facchinetti[3]

[1] INRAE: National Research Institute for Agriculture, Food and the Environment, France
[2] POLIMI: Politecnico di Milano – DEIB, Milan, Italy
[3] UNIMI: Università degli Studi di Milano – DISAA, Milan, Italy

* Corresponding author: <manon.boulet@inrae.fr>

Abstract: METRICS is an EU-funded project dedicated to the metrological evaluation and testing of autonomous robots. ACRE is one of the four benchmarking competitions for autonomous robots and smart implements organized by METRICS. ACRE deals with the applications of robotics to agriculture. The participants are required to execute performance benchmarks, which are grounded on the concepts of objective evaluation, repeatability, and reproducibility. Transferring such concepts in the agricultural context, where large parts of the test environment are not fully controllable, is one of the challenges tackled by ACRE. ACRE is focused on agricultural tasks such as weeding or mapping/surveying crops down to single-plant resolution. Seven benchmarks were identified and classified in two categories.

ACRE competition involves two separated interconnected events: a Field Campaign that involves robots executing activities in agricultural environments such as open-air experimental plots, and a Cascade Campaign during which Artificial Intelligence systems perform activities on data collected during the Field Campaigns.

Two dry-run evaluation campaigns took place in 2020 and 2021. These two first events called "dry-run evaluation campaigns" allowed to test, check, complete and validate the ACRE organization with its evaluation plan. The first field evaluation campaign began with an on-field event from 7th to 10th June, 2022. A second cascade evaluation will take place at the beginning of 2023 and a last field evaluation campaign of the project is scheduled to take place in May 2023, in Cornaredo, near Milan, in Italy.

Keywords: test, digital agriculture, robotics and automation, performance evaluation, sustainable agriculture

I. INTRODUCTION

METRICS [1] is a European project dedicated to the metrological evaluation and testing of autonomous robots in four Priority Areas, for which competitions are organized. Among these four competitions, ACRE [2] deals with the applications of robotics to agriculture. Like the other three competitions, ACRE is a competition based on the benchmarking method with the goal of exploiting the appeal and desirable features of competitions to foster a benchmarking culture in European robotics. Several competitions have already been organized prior to the creation of ACRE. However, only one competition has already dealt with robotic weeding, the ROSE challenge [3].

The ROSE challenge was a French project, which began in 2018 and was co-led by the National Laboratory of Metrology and Testing (LNE) and the National Research Institute for Agriculture, Food and the Environment (INRAE). It ended in June 2022, after four field campaigns during which four consortia teams developing weeding robots competed. The main goal of this challenge was to encourage the development of innovative solutions for intra-row weeding to reduce or even eliminate herbicide usage. This challenge provided the ACRE organizers with knowledge and experience regarding the evaluation of robots on the field: the evaluation methods, image processing with the DIANNE (Clipping, Identification and ANNotation for Evaluation) software developed by LNE, the metrics used, in particular the EGER (Estimate Global Error Rate) metric which takes into account the error rates of each participant based on manual counts by the organizers before and after the weeding action.

ACRE follows the model of the ROSE challenge with field evaluation campaigns followed by cascade evaluation campaigns. This type of organization is dependent on weather conditions to prepare the field evaluations, which implies that the organizers must plan the interventions on the plots in order to obtain plants at the necessary stages of development for the good evaluation of each team on the selected benchmarks.

II. THE ACRE ORGANISATION

A. The ACRE framework

1) Experimental context

The METRICS project aims to organize challenges in the four Priority Areas (PAs) defined by the European

Commission: Inspection and Maintenance (I&M), Agile Production, Healthcare and Agri-Food to evaluate robots through several competitions. Among the four PAs of this project, ACRE aims to evaluate robots on different agricultural applications. The opportunity to evaluate robots dedicated to weed control is part of a dynamic that tends to reduce or even eliminate the use of phytosanitary products in the field.

2) Competition methodology

The METRICS common framework focuses on providing methods to maximise the reproducibility of evaluations. These specific methods are for identifying and controlling influencing factors, measuring the environmental conditions (brightness, temperature, wind, soil conditions, etc.) and describing the test environments (objects to be recognised and handled, furniture and wall layout, test database, etc.). The robots are evaluated through several selected benchmarks; they have to perform well-specified tests in realistic environments or on databases, and their performances are assessed by applying quantitative metrics.

B. The ACRE evaluation campaigns

The ACRE competition is divided into two separate but interconnected tracks. The first one includes the Field evaluation campaigns which involve robots performing activities in an agricultural environment. The events of the second track are called Cascade evaluation campaigns: in these, Artificial Intelligence systems perform activities on data generated and collected during the Field Campaigns. The ACRE evaluation campaigns happen every year, with two dry-run evaluation campaigns in 2020 and 2021 and a first official evaluation campaign in 2022, the second and last campaign will take place in 2023.

1) The field evaluation campaigns

Due to the issues caused by the COVID-19 pandemic, only one participating team from the ROSE challenge signed up for the first ACRE dry-run Field evaluation campaign organised in October 2020. Therefore, to have more hindsight regarding the protocols established in the evaluation plan redacted in 2019 [4], instead of the first Field evaluation, another dry-run Field evaluation campaign was scheduled for June 2021 but had to be postponed to September 2021 due to unfavourable weather conditions. This campaign had four participating teams who signed up for various benchmarks depending on their robot's abilities.

After these two dry run evaluation campaigns, the protocols were adjusted thanks to the results gathered during the testing of each benchmark. Then, the first official field evaluation campaign was planned for June 2022. This time around, five teams participated in the benchmarks.

Both dry-run evaluation campaigns as well as the first field evaluation campaign took place at the INRAE site of Montoldre (France). The second and last field evaluation campaign is scheduled to take place in May 2023 in Cornaredo, near Milan (Italy).

2) The cascade evaluation campaigns

For the cascade evaluation campaigns, the set of possible benchmarks is limited to pure perception, that is, Plant discrimination. The cascade evaluation campaigns are scheduled to happen a short time after the associated field evaluation campaigns, and last for about three months.

III. THE ACRE FIELD EVALUATION

A. The experimental field design

1) The set up experimental plots

The experimental field is divided into several kinds of plots in accordance with the needs of each evaluation and provided by the ROSE challenge experience. Most of them are left with natural weeds, with an inter row hoeing work performed before the evaluations, but the weeding benchmarks require that four selected weeds be sown in the crop's intra row space for consistent evaluation of all participants.

The plots of 2 meters of width and 46.5 meters of length are prepared and sown about three weeks before the evaluations, which are scheduled every year for late May or early June, if the weather conditions are favourable.

For the specific Field navigation evaluation, the robots are tested on their ability to follow a trajectory without damaging the crop plants with only selected reference GPS points on a specific experimental plot. On a part of the plot, an offset of 37.5 cm is applied on the straight rows of crops, over a length of 15 meters, before getting back on the original straight row.

Moreover, for the Crop mapping evaluation, a randomized sampling of plants needs to be performed to test the robots' ability to create a map of a plot with variable density.

2) Selected crops and weeds

Taking advantage of the experience acquired during the ROSE challenge, the organizing consortium of ACRE had decided to keep the same crops and weeds they had used in the previous challenge. For the type of crops sown, it was decided that two kinds were needed: one with a wide inter-row spacing and the other with a smaller inter-row spacing, like a vegetable crop. For the ROSE challenge, maize and bean were the selected crops. Maize was sown in two rows, with an inter-row of 75 cm and 14 cm between each plant on a row. As for bean, it was sown in three rows, with an inter-row space of 37.5 cm and 7 cm between each plant on the row. Four types of weeds were selected for the ROSE challenge and kept for the ACRE campaigns: mustard, rye grass, chenopodium and matricaria. These four weeds were sown in the 10 cm wide intra-row space, centered on the seeding row, at a density of 27 weeds by linear meter, allowing for a diversity on the field adapted to the evaluation of the robots' ability to weed different kinds of plants. In accordance with the ROSE challenge execution, the plot organisation on the experimental field was maintained.

B) Benchmarks deployed

ACRE's benchmarks take two forms. Functionality Benchmarks (FBMs) are focused on specific capabilities of a robot and are designed to make the benchmark as independent as possible from robot components not directly involved in the functionality under examination. Task Benchmarks (TBMs) combine multiple Functionalities for the execution of complex activities and the result depends both on the individual functionalities and on the integration between components.

An evaluation plan gathers all information regarding the ACRE benchmarks with details on their execution and evaluation metrics. The benchmarks involve three different robot capabilities required in agricultural applications: robot perception, navigation, and manipulation.

1) The Functionality Benchmarks (FBM)

For all the functionality benchmarks except for the specific Field Navigation benchmark, the robots are not required to move autonomously.

The first benchmark called Plant discrimination deals with robot perception capability of crops and weeds. During this task, the robot is evaluated on its capability of discriminating which plants of a row are weeds and which are crops (intra-row detection). The robot is required to make a pass over a prepared row containing both crops and weeds using its sensors. Then, the robot classifies the crops and weeds present in the rows.

The Leaf area estimation benchmark is an evaluation of a robot's capability to estimate the plants' leaf area along a cultivated row. The robot must move along the row and use its perception capabilities to estimate the variable leaf area along the entire row.

Another estimation benchmark is Biomass estimation. It evaluates the capability of estimating aboveground crop biomass. The robot must make a pass over a prepared field composed of one or more rows, using its sensors to perceive the plants. The robot must estimate the fresh weight of the aboveground parts of the plants without distinguishing between crops and weeds.

The Field Navigation benchmark deals with a robot's capability to navigate along a prepared plot without damaging the crop. The prepared plot is divided into three parts: one first part of it in a straight line, while a second part includes a row shift of 37.5 cm on the crop rows, then the third and last part is in straight line. The robot under test has only the GPS reference points to reach the end of the course without damaging the crops with as much accuracy as possible compared to the reference trajectories acquired during the sowing of the field.

The last FBM, Weed Destruction, is an evaluation of a robot's capability of destroying weeds in the intra-row without damaging the crops. The evaluation compares the state of the test plot with manual counts before, immediately after and a few days after the weeding operations. To make this evaluation as independent as possible from other functionalities, coloured markers are used to identify crop and weed plants in the prepared plot.

2) The Task Benchmarks (TBM)

For the two task benchmarks, the robots are required to move autonomously.

The Crop Mapping task is the evaluation of a robot's capability to produce a map of the entire cultivation area by exploring it autonomously. The robot must explore a multi-row cultivated plot and provide a map of crop plants. It has to recognize single plants and provide their positions on a Cartesian coordinate system.

The second and last TBM is Intra-Row Weeding. This benchmark assesses a robot's capability to perform fully autonomous intra-row weeding of a row of crops. The robot must eliminate the weeds located among crop plants without damaging the crops. No coloured markers are used on the plants to facilitate their detection and identification.

C) The off-field data analysis

After the evaluations on the field, the results are gathered and analysed.

For the Field navigation evaluation, a R script [5] was redacted to compare the trajectories of each participant with a reference trajectory obtained during the sowing a few weeks before the evaluations. All trajectories were obtained using a laser tracker device. A magnetic target with a mirror is installed on each robot to receive the laser beam emitted by the tracker. When the laser beam is reflected, a relative position of the target is recorded. Afterwards, in post treatment, using the absolute GPS coordinates of the position where the tracker is set up, the absolute GPS coordinates of each trajectory can be deduced from it, generating the trajectories files. The obtained trajectories can then be compared to the reference as well as between each participant. Using the ggplot2 R package [6], the graph of Figure 1 shows the field navigation results obtained for the straight bean plot during the first field evaluation campaign in June 2022.

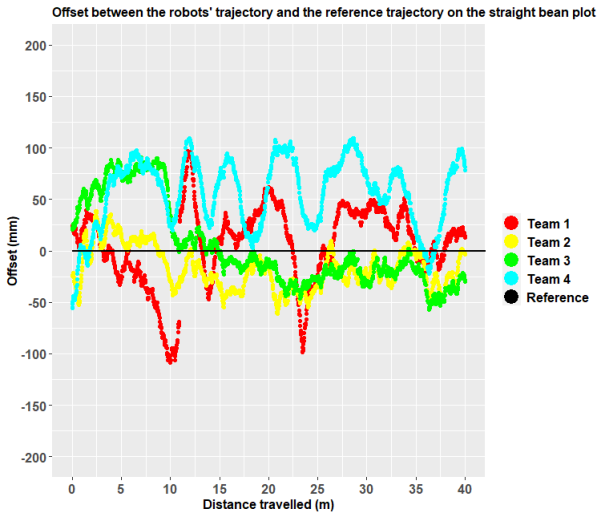

Figure 1. Field navigation results for the straight bean plot during the first field evaluation campaign in June 2022

The reference trajectory recorded during the sowing is the black line and is to be compared with data gathered for the four participating teams. For each recorded trajectory, the offsets, the smallest and the largest deviations can be looked into and analysed. The obtained results are different between the four solutions of each participant team. The maximum measured offsets are more than 100 mm. These field navigation results obtained on the same straight bean rows show the progress that has yet to be made for a precise autonomous navigation.

The Crop mapping evaluation requires the organizing team to perform a randomized sampling on the plot before the participants make a pass on it. The evaluators record the positions of the remaining plants on the rows and the participants must send the plants' positions they collected with their robots. Then, both datasets are compared and the accuracy of the participating team is assessed. The prepared Crop mapping evaluation plot was not used because of a lack of participants for this benchmark.

The weeding actions are also analysed after the field evaluations using the manual counts results obtained before and after each weeding action.

The data for this evaluation have been acquired through manual counts at three dates. June 8th was two days before the weeding action was performed. On June 10th, the one robot participant made only a part of a pass on the plot and the organizers counted the destroyed or uprooted crop plants and weeds. A last manual count was performed on June 15th, a few days after the weeding action, to check if the crop plants and weeds had shown respectively signs of death or re-growth.

Figure 2. Intra-row weeding results on the bean/rye-grass plot for the only team who participated

The data are compiled and allow obtaining error rates on weeds that were not destroyed and on crop plants that were damaged or uprooted. Figure 2 shows the intra-row weeding results obtained for the only team that partially participated on the bean/rye-grass plots during the first field evaluation campaign in June 2022. These few results show the need for improvement in this field.

IV. THE ACRE CASCADE EVALUATION

A. General framework

The ACRE Cascade Campaigns are online competitions targeted at researchers and practitioners in Artificial

Intelligence, where the organizers ask the participants to segment RGB images to distinguish between crops, weeds, and background. There has been a dry-run Cascade Competition in the winter of 2020 and the first Cascade Campaign in the spring of 2022. The data for the competitions came from the ROSE challenge. In particular, in the dry-run cascade competition, the organizers asked the participants to segment the ROSE images collected in 2019, while the first Cascade Campaign focused on domain adaptation. Thus, the main goal was to segment the images of the year 2021 by training the models on the images of the year 2019. A generalization capability of the models, that is to be trained on a Source domain and achieve good performance in a Target domain, is of fundamental importance for adopting the technology by real users.

B. Competition platform and dataset

Both competitions have been hosted on the CodaLab platform that provided all the tools to manage the request of participations, the distribution of the datasets, and the evaluation of the submissions. The dataset was composed of images collected during the ROSE Challenge campaigns and captured by different sensors at different moments, and was about two kinds of crops: maize and bean. Data came specifically from the 2019 and 2021 ROSE challenges, where four teams (BipBip, Pead, Roseau and WeedElec) competed with agricultural robots. Each team has collected images of the same two crops, but at different moments and with different sensors (all are RGB cameras). The dataset contained both RGB images and labelled masks (ground truth). Human annotators have produced the labels under the supervision of LNE. Masks were composed of three different classes: crop, weed, and background. Figure 3 shows an example of an RGB image and its corresponding labelled mask.

Figure 3. A couple of RGB image
and corresponding ground truth mask from the dataset
used in the 2022 ACRE first Cascade Campaign

Dataset images were divided by the team that acquired the image, and for each team, by the type of crop present in the images, i.e., maize and bean. For the first Cascade Competition, the task was focused on the domain adaptation between different years and not different sensors. In Figure 4, it is possible to appreciate the significant difference in colour, perspective, and field of view in the datasets of the four teams. Indeed, each of the ROSE teams has chosen a different positioning and setting for the camera used in the plant/weed discrimination.

Figure 4. Samples of images captured by the different teams
at the 2019 ROSE Campaign.
From top to bottom, left to right, BipBip, Pead, Roseau, WeedElec

In addition, lighting conditions are quite different, as some teams have decided to structure as much as possible the lighting conditions. In contrast, other teams have placed no specific care on the lighting of the scene when acquiring the images. For these reasons, for the first Cascade Campaign it was decided to only provide the images from the two BipBip and WeedElec teams, that showed the highest similarity.

C. Evaluation

Participants were evaluated on the mean Intersection over Union (IoU) obtained on the two classes, crop and weed. The Intersection over Union, also called Jaccard Index, is typically used in segmentation tasks, and it essentially quantifies the percentage of overlap between predicted and target segmentations. If A is the prediction and B is the ground truth, the IoU is calculated as in the following:

$$IoU = \frac{A \cap B}{A \cup B}$$

The area of the intersection contains the True Positive (*TP*) pixels. The union is computed as the sum of prediction's pixels not overlapping with the ground truth (False Positives – *FP*), of the intersection (*TP*), and of ground truth pixels not overlapping with prediction's pixels (False Negatives – *FN*).

IoU was computed for each target class (crop and weed) separately by considering prediction and ground truth as binary masks. Then, the final IoU is calculated by averaging the two. Thus, this was the formulation:

$$IoU_{crop} = \frac{TP_{crop}}{TP_{crop} + FP_{crop} + FN_{crop}}$$

$$IoU_{weed} = \frac{TP_{weed}}{TP_{weed} + FP_{weed} + FN_{weed}}$$

$$IoU = \frac{IoU_{crop} + IoU_{weed}}{2}$$

Where *TP* are the True Positives, *FP* are the False Positives, and *TN* are the False Negatives.

Thanks to the CodaLab Competitions framework's flexibility, it was possible to score the participants with different customized IoUs. In particular, the participants were scored according to the Global IoU (by considering the images of both crops and the four teams), and the Maize and Bean IoUs. Thus, three competition winners for each category were nominated.

D. Results of the first Cascade Campaign

The first Cascade Campaign lasted from February 23rd 2022, to May 21st 2022, and it has been divided into three phases, Development, Generalization, and Final.

In the Development phase, participants were asked to develop a model to perform semantic segmentation of RGB images, that is, to distinguish crop, weed, and background pixels. Participants received a training dataset with images of the year 2019 and were asked to predict on a test set of images again of the year 2019.

In the Generalization phase, participants were asked to submit predictions on the first part of the new unlabelled 2021 dataset by using their models trained on the 2019 dataset.

In the Final phase, participants were required to submit predictions of the second part of the 2021 dataset. This stage was thought to submit the final model without major changes; thus, the duration was limited to three days and the number of submissions to three. The limit to the number of submissions was imposed to reduce the risk of overfitting. Overfitting happens when models are fitted too closely to a set of data, and therefore they cannot generalize well on new unseen data. By limiting the number of submissions in the Final phase, the possibility of participants to fit their models too closely to the Test data was limited.

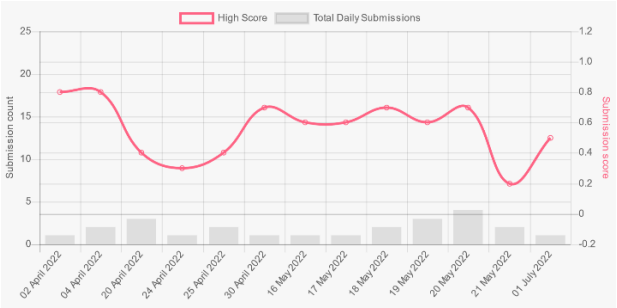

Figure 5. Daily-wise distribution of the total number of submissions and evolution of the daily highest score (Global IoU)

The highest Global IoU was 0.83 in the Development phase, 0.68 in the Generalization phase and 0.69 in the Final phase. In the Development phase, the highest IoU related to Bean and Maize were 0.82 and 0.84. In the Generalization phase, the highest IoU related to Bean and Maize were 0.67 and 0.69. In the Final phase, the highest IoU related to Bean and Maize was 0.69 for both categories. The results are summarized in Table 1.

Table 1. Best IoU results for each phase and each type of evaluation

	Global IoU	Bean IoU	Maize IoU
Development	0.83	0.82	0.84
Generalization	0.68	0.67	0.69
Final	0.69	0.69	0.69

The results obtained in the Generalization and Final phases were lower because the algorithms have only a limited capacity to segment images of a new domain. Bean and Maize images did not show relevant differences in the corresponding IoU scores, suggesting a similar task complexity.

V. CONCLUSION

The METRICS project gathers a set of competitions in four Priority Areas, among which is the Agri-food Competition for Robot Evaluation, ACRE.

Since 2019, the organizers of this project have worked on establishing and testing a variety of protocols applied in evaluation campaigns of robots dedicated to agricultural use. These protocols originated from the INRAE experience of the ROSE Challenge.

The protocols that were established and written in an evaluation plan in 2019 were then adjusted as the campaigns went on. Each campaign, from the first dry run to the first official campaign, has allowed to test and improve the protocols and methodologies.

Although one of ACRE's main evaluation fields is to evaluate robots' weeding capabilities, most of the participants took part only in the Field navigation evaluation. Only one team performed the weeding tasks and was evaluated on a portion of the plot. Due to technical issues, they could not perform the entirety of the task.

The teams who participated in the different campaigns have used this opportunity to identify their shortcomings and know in which field their autonomous solutions need improvement.

The last campaign, in Italy, will be a new challenge in itself; weather conditions will be different from the ones encountered in France. Moreover, the soil type is different, and the crop species are supposedly different as well. These modifications will complement the results already obtained by accumulating diversity and therefore will allow to increase the robustness and reliability of the results and of the established protocols.

The main goal of the ACRE organizing team is now to take advantage of this accumulated experience and use it for the last campaign of 2023 in Italy, as well as for possible future challenges and projects.

REFERENCES

[1] METRICS, *Metrological evaluation and testing of robots in international competitions*. [Online]. Available: <https://metricsproject.eu/>

[2] ACRE, *Agri-food competition for robot evaluation*. [Online]. Available: <https://metricsproject.eu/agri-food/>

[3] The ROSE challenge. *RObotics and Sensors for Ecophyto*. [Online]. Available: <http://challenge-rose.fr/en/home/>

[4] ACRE evaluation plan. [Online]. Available: <https://metricsproject.eu/wp-content/uploads/2020/07/Submitted-deliverables_M7_METRICS-deliverable_D5.1-ACRE_evaluation_plan_post-review2.pdf>

[5] R Core Team (2022). R: *A language and environment for statistical computing*. R Foundation for Statistical Computing, Vienna, Austria. <https://www.R-project.org/>

[6] H. Wickham. ggplot2: *Elegant Graphics for Data Analysis*. Springer-Verlag, New York 2016.

Experimental Evaluation of Path-Tracking Control Strategies for an Agricultural Tracked Robot 8th International Conference on Machine Control & Guidance

Luc Desbos[1]*, Christophe Debain[2], Caroline Acanfora[1], Jean Laneurit[2], Philippe Heritier[2], and Roland Lenain[2]

[1] Agreenculture, 31400 Toulouse, France
[2] Université Clermont Auvergne, INRAE, UR TSCF, F 63178 Aubière, France

* Corresponding author; <luc.desbos@agreenculture.fr>

Abstract: This paper deals with an experimental evaluation of several path-tracking control methods for tracked vehicle. We present adaptive strategy, allowing to take into account the phenomena of slipping occurring over the robot. Different observers algorithms are used to estimate these slip parameters in real time. To anticipate the trajectory turns, predictive method such as feedforward and MPC are introduced. The low-level controller problem is also addressed. We present two strategies to ensure the control of longitudinal and angular velocities of the robot. All these approaches are applied to Ceol, a tracked robot used for vineyard crop maintenance. Full-scale experiments are presented under various conditions. We tried and tested these methods on a regular flat field, on a slope but also in a real vineyard with an implement working the soil.

Keywords: path-tracking control, experimental study, nonlinear control, predictive control, adaptive control, agricultural tracked robot, vineyards weeding

I. INTRODUCTION

The constant increase of the population has created needs in food production. On the other hand, the use of chemicals must be reduced to limit environmental impacts. Mobile robotics is emerging as a new solution to make agriculture sustainable while maintaining the necessary production. Robots free up farmers time, they act regularly and autonomously by carrying out mechanical treatments in the crops. Instead of using large tractors, small tracked robots are designed to reduce fuel consumption and pressure applied to the soil, resulting in higher yields (Tomis et al. 2014). However, robotics still has a major technological challenge to overcome before it can become a permanent part of the agricultural ecosystem: making robot guidance robust and safe. Several researches projects have been conducted on path-tracking control strategies, but most of them concern wheeled robots. Finally, there is a lack of papers addressing the problem of path-tracking for tracked vehicles and performing full-scale experiments.

In the literature, the control architecture is generally composed of two controllers. The first one, named high-level controller, computes the longitudinal and rotational velocities based on the localisation errors to converge to the trajectory. The second one, called low-level controller, ensures that the velocities from the high-level controller are followed by the robot. We retain this structure in this work. There are many methods to design a high-level controller. First ones were based on geometric principles such as the "follow the carrot" or "pure pursuit" strategies (Wit et al. 2004). The backstepping technique appeared in 1992 (Kokotovie, 1992). It was first applied to a wheeled robot in simulation (Fierro and Lewis 1997). Then, we started to add observers and to design adaptive control (Wang et al. 2004; Moosavian and Kalantari 2008; Dar and Longoria 2010; Lenain et al. 2017). These updates take into account the slippage occurring when the robot evolves off-road, at higher speed, or during turns. Furthermore, robots do not have instantaneous response time, and this phenomenon must be anticipated when the path curvature change. To this end, predictive control has been widely used (Kanjanawanishkul et al. 2009; Picard et al. 2020). Other high-level strategies are based on neural-network (Gu and Hu 2002; Xiao et al. 2017; Shi et al. 2016) or on optimization problem (González et al. 2011) but they are time and memory consuming.

In this paper, we address the problem of path-tracking applied to Ceol: the Agreenculture crawler. The paper is divided as follows. First, two low-level controllers using classical control strategy are presented. Then kinematic model and extended kinematic model are recalled. Based on the second model, different observers are introduced: A classical backstepping controller is implemented to serve as a reference. Compared to the backstepping, we design different adaptive and predictive control. Finally, a wide scope of experiments over Ceol are presented and analysed in many situations in order to test the effectiveness of developed strategies.

II. LOW-LEVEL CONTROLLER

The low-level controller has the purpose to ensure the correct control of longitudinal and angular speed. Velocities of right and left tracks are then controlled by the two inverters of Ceol. To resume, we have to compute left and right tracks speed in order to guarantee that setpoints of high-level controllers are reached. In our case, we chose to regulate only the angular speed because we are quite sure of our longitudinal speed model. Moreover, the regulation did by the inverters is sufficient to ensure the required performance over longitudinal velocity. About angular speed regulation, two methods have been implemented and tested. The first one is a simple PID, based on the error between the angular speed ω calculated by the high-level controller, and the angular speed measured ω_M by the IMU. This measurement has to be debiased and filtered. The second one is what we called a P + ID. It is an alternative to the PID which consist of applying the gain k_p directly to the setpoint and not to the error state. By doing this, we include a bit of model into the controller, and it helps to improve responsiveness. Equations of these two regulations approaches are as follows:

$$\omega^C_{PID} = k_p(\omega - \omega^M) + k_i\int_0^t(\omega - \omega^M)dt + k_d\frac{d}{dt}(\omega - \omega^M)$$

$$\omega^C_{P+ID} = k_p\omega + k_i\int_0^t(\omega - \omega^M)dt + k_d\frac{d}{dt}(\omega - \omega^M) \quad (1)$$

Angular and longitudinal velocities are used in the geometrical model of Ceol, to compute a left V_l and a right V_r track speed. In the case of the crawler, we take the same model as a skid-steering robot. Defining ω_C as the angular speed output of the PID or P + ID, velocities are computed as follows:

$$V_r = v + \frac{b}{2}\omega^C$$
$$V_l = v - \frac{b}{2}\omega^C \quad (2)$$

Finally, the low-level controller global structure is:

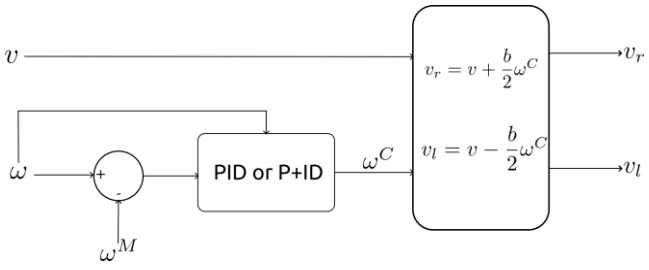

Figure 1. Low-level controller

Both of these architectures has been tested with Ceol on different kind of soil. The settling time of the longitudinal speed has been calculated at 0.7s, with no steady-state error. With a longitudinal speed of 0.5m/s, we measure a settling time of 1.5s for the angular speed with PID, and of 1s with P + ID strategy (Figure 2).

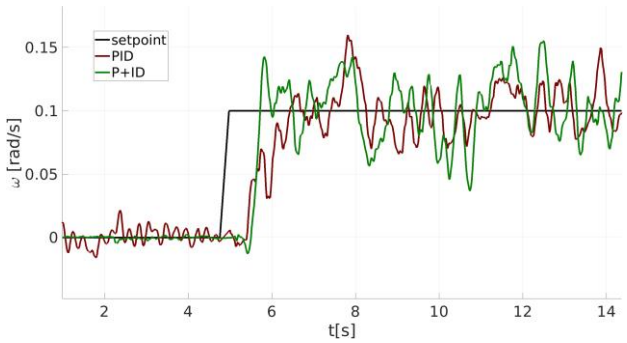

Figure 2. Angular speed response

III. HIGH-LEVEL CONTROLLER

In this section, we rely on scientific literature to design the complete high-level controller.

A. Modelling and observation

The kinematic model is established with the work (Morin and Samson 2008). Frenet frame is used as a base to locate the robot position on the trajectory (Equation 3). We define s as the abscissa curvilinear, y as the lateral deviation and $\dot{\psi}$ as the angular deviation. All these variables compose the model.

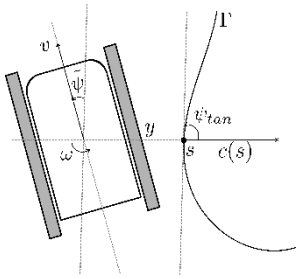

$$\begin{pmatrix}\dot{s}\\ \dot{y}\\ \dot{\tilde{\psi}}\end{pmatrix} = \begin{pmatrix}\frac{v\cos(\tilde{\psi})}{1-cy}\\ v\sin(\tilde{\psi})\\ \omega - \frac{cv\cos(\tilde{\psi})}{1-cy}\end{pmatrix} \quad (3)$$

In order to take into account the slippage that the robot undergoes, we add some parameters in our model to create an extended kinematic model. These parameters can be expressed in skid model form, with a perturbed longitudinal speed v_p, a sideslip angle β and a yaw rate perturbation $\dot{\tilde{\psi}}$. Or, they can be in generic form, with a perturbation on each coordinate of the Frenet frame:

$$\begin{pmatrix} \dot{s} \\ \dot{y} \\ \dot{\tilde{\psi}} \end{pmatrix} = \begin{pmatrix} \dfrac{(v+v_p)\cos(\tilde{\psi}+\beta)}{1-cy} \\ (v+v_p)\sin(\tilde{\psi}+\beta) \\ \omega - c\dot{s} + \dot{\tilde{\psi}}_p \end{pmatrix} = \begin{pmatrix} \dfrac{v\cos(\tilde{\psi})}{1-cy} + \dot{s}_p \\ v\sin(\tilde{\psi}) + \dot{y}_p \\ \omega - c\dot{s} + \dot{\tilde{\psi}}_p \end{pmatrix} \quad (4)$$

To evaluate these new slipping parameters, we introduce three observers. The first one is based on backstepping technique (Bouton et al. 2007), the second one on Lyapunov technique (Lenain et al. 2017), and the last one on super-twisting observation theory (Nagesh and Edwards 2013). Detailed descriptions of them can be found in given references. In our work, we implemented the backstepping observer to evaluate sliding expressed in skid model form, super-twisting observer to evaluate slip expressed in generic form and Lyapunov observer to evaluate sliding expressed in both form.

B. Control

The first approach to design a high-level controller is to use the backstepping technique. Based on (Deremetz 2018), the controller is decomposed in two part. The first one computes a desired heading ψ_d which the robot has to follow to converge to null lateral deviation e_y. The second one computes the associated yaw rate ω to match ψ_d, considering the actual heading, and the curvature of the path.

$$\omega = k_\psi \left(\tilde{\psi} - \arctan\left(\frac{k_y e_y}{1 - v(s)y} \right) \right) + c\frac{v\cos(\tilde{\psi})}{1-c(s)y} \quad (5)$$

Gains k_y and k_ψ must be tuned to set the dynamic of the robot. This controller is based on the kinematic model of robot, thus, sliding parameters can be included in the equation to design adaptive control strategy (see (Lenain et al. 2017) for an application with Lyapunov observer).

Any robot has a dynamic response which is not instantaneous and should be considered. These dynamics introduce some delay in the command which will be compensated by the predictive control. We consider two strategies in this work: feedforward and LMPC (Lenain et al. 2006).

Feedforward method uses the curvature among the robot on the path in the command equation. We define ff as the time of prediction used to determine this curvature. It permits to anticipate the future trajectory curvature.

The technique that we recalled LMPC is based on model predictive control. In this strategy, an approximated second order model is used to modelling the low-level of the robot. The command minimize deviation over a horizon H between predicted and desired angular speed to anticipate the low-level behaviour.

IV. EXPERIMENTAL RESULTS

A. Experimental setup

Experimental studies have been conducted with Ceol from Agreenculture society. This crawler has a weight of 700 kg and is designed to work in vineyard. The 3-point linkage at the rear of Ceol, permits to carry usual agricultural implement till 500 kg. In these experiments, we test the algorithms with a shredder of 250 kg (Figure 3) used to cut the grass of the intra-row of the field. Also, we test the guiding with a carried frame of 200 kg having two inter-vines hoe (Figure 4). This frame weeds rows of the field, without damaging any vine stock.

Figure 3. Schredder

Figure 4. Carried frame with inter-vine hoe

Ceol has a AGCbox, which computes the precise localisation of the robot, and sends this information on a CAN bus. AGCbox also communicates its IMU data. A computer running ROS (Robot Operating System) is as well connected to the CAN bus. This computer gets all the information of the robot (odometry data) and of the AGCbox, and runs low-level and high-level controllers. The first one is running at a frequency of 50 Hz whereas the second is running at 10Hz. This architecture allows to guide the robot accurately, using localisation of AGCbox.

Table 1. Gains parameters in function of velocity

Velocities	kp	k_d	ff	H
0.7 m/s	–0.5	–1	–	–
1 m/s	–0.26	–0.8	–	–
1.5 m/s	–0.23	–2.5	0.3	15
2 m/s	–0.1	–2.5	0.8	40

For all of these experiments, we work a lot on tuning our gains: for prediction, adaptation, observers, etc. Some gains depend on the velocity of the robot, they are summarized in Table 1.

Furthermore, we use gains for low-level model identification and LMPC, which stays the same for different speed. Also, we use the P + ID low-level controller with constant gains k_p and k_i. They are all summarized below.

Table 2. Prediction parameters

a_0	a_1	b_1	b_2	α	kp	k_i
0.02372	0.01088	1.529	-0.5636	0.9	0.6	1.2

For analytical purposes, most of the next presented curves represent the lateral deviation of the robot in comparison to its trajectory. These curves are expressed in function of curvilinear abscissa. Grey colour of graphics indicates zones where curvature of the reference trajectory is not null.

B. Impact of adaptive control

Adaptive control improves system performance when a lack of adherence occurs. In this paper, we try to highlight benefits of this strategy, testing algorithms on a slope, during turn and when the robot is weeding a field.

1) Guiding on a slope

First experiment[1] has been conducted at 1m/s in a harvested wheat field, where the slope evolves between 20% and 45% and the soil is quite hard. The purpose was to see the effectiveness of adaptive control in a situation of important slope. The trajectory to follow (Figure 5) is a straight line of 50 m followed by a turn with a radius of curvature of 5 m, and another straight line.

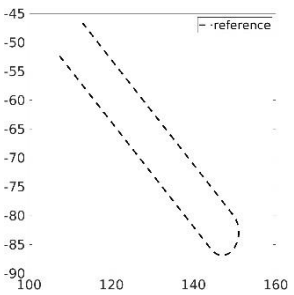

Figure 5. Trajectory on the slope

Figure 6. Experimental setup

[1] A video of the experiment is available at: https://youtube.com/shorts/ZE-4kcbLhyM

The robot is push to its left during the first straight line and to its right on the second one. During the curve, the robot turns into the slope. It is probably the case generating the most slippage because the inertia and the slope effect are acting in the same direction.

We tried to follow this trajectory with a simple backstepping, and then to add observers estimations to the command. Results are as follows (Figure 7).

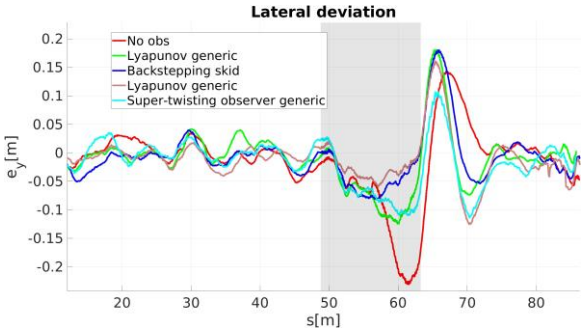

Figure 7. Comparison of adaptive strategies on a slope

During the straight motion, the lateral deviation is oscillating around 0 even without adaptive control. Visually, we noticed that Ceol did not slip even on an important slope that could be a risk for its integrity. On that kind of soil, tracks are effective enough to limit slip. Adaptive control does not significantly improve performances on straight lines, because the slip is not important. Conversely, they tend to add noise to the command. At the end of the bend, the backstepping suffers from an overshoot of 25 cm. At the same place, the use of observers by adaptive approaches permits to reduce the overshoot from 25 cm to 10 cm. In fact, this zone is the most critic of the trajectory. Due to the slope and its inertia, the robot slip in direction of the slope. Adaptive control detects and compensates the slip to improve performances of the path-tracking. All the observers seems equivalent, none of them stands out with much better performances. The rising pic at the end of the turn can be explained by the lack of prediction in the command.

2) Permanent turning

The second experiment is conducted on a flat regular field. The trajectory (Figure 8) is constituted of a straight line of 30 m and then a turn of constant radius of 5 m during 200 m. We speed up to 1 m/s with and without implement.

Adaptive control is tried to see the impact of its utilisation when using various robot configurations. Results are presented in Figure 10.

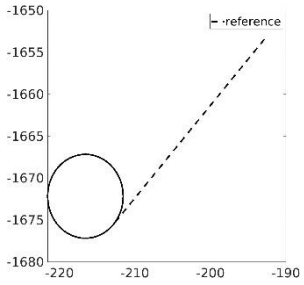

Figure 8. Trajectory of permanent turn

Figure 9. Experimental setup

During the steady-state of the turn, the lateral error of the experiment without implement (red curve) is more centered than for the experiment with implement (blue curve). We explain that phenomenon by the distribution of masses over each track. Naturally, Ceol mass is concentrate on the front of the tracks. Adding a heavy implement as a shredder distribute the masses and the pressure uniformly over the tracks. Thus, the kinematic model used for control is more realistic than without shredder. When we are looking at the results with adaptive control (green without implement, brown with implement), there is no more difference, and they are both of them centered. Adding observers compensate the model uncertainties.

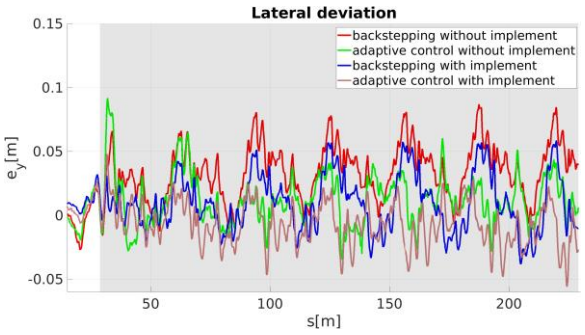

Figure 10. Comparison during permanent turn

3) In a vineyard environment

This experimentation[2] took place in a vineyard in the south of France. The purpose was to test algorithms in real conditions of weeding work in a nominal environment. The implement used is a carried frame with inter-vine hoe. There is a mechanical sensor touching vine stocks to detect and avoid it. It permits to work as close as possible to every vine stock. But this implement creates a lot of disturbances (continuous and punctual) over the robot, especially when the sensor touch and release a vine stock. The plot in question had not been worked for a long time. Experiments are realized at 0.7 m/s in vine row of 70 m.

Figure 11. Trajectory vineyard

Figure 12. Experimental setup

We are comparing performances of path-tracking in three different cases. First case is when the robot just carries its implement in the row without working. The second case is when the robot works a row for the first time. In this case, there are indeed a lot of disturbances. Finally, the third case is when the robot is doing nominal work, after more than three passages working on the same row. We are showing results with backstepping approach Figure 13. Even if we do not use them in the command, outputs of Lyapunov observer are presented Figure 14.

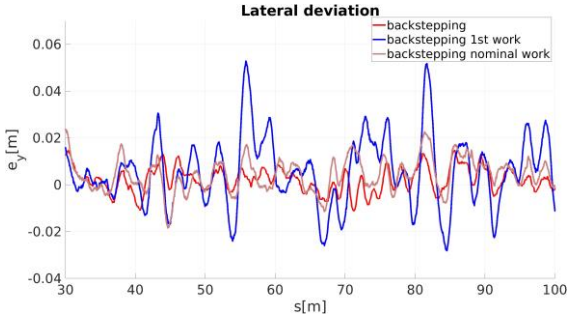

Figure 13. Working in vineyard conditions

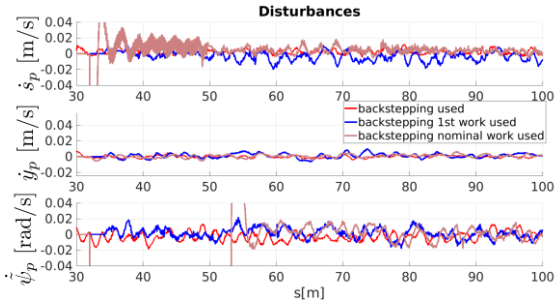

Figure 14. Perturbations during work

Red curve in Figure 13 shows that when the robot does not work the soil, performances are quite good. Lateral deviation oscillates around 0 with a precision of ±1 cm. During first work on the lane (blue curve), the

[2] A video of the experiment is available at https://youtube.com/shorts/VwRTeUsAX4o

implement has a lot of work to do, which create a lot of perturbation over the guiding. Results are quite bad, because some pics reach 6 cm of lateral deviation. Nevertheless, the robot was able to achieve its task without damaging any vine stock. Finally, on a more nominal task (brown curve), results are not as good as without working, but, they are totally satisfying. The robot oscillates around 0 with a precision of ±1.5 cm. Looking observers results (Figure 14), we are not seeing any difference between the experiment in nominal work condition, or without working. A slight difference is noticeable during the first work on the row, especially on $\dot{s}_p$. This means that observers only see disturbances affecting longitudinal velocity, and cannot detect punctual lateral perturbations, which are the main concern of our problem. Thus, adaptive control is useless to improve performance of path-tracking during a harsh weeding work.

C. Impact of predictive and adaptive control

Adding prediction term into command allows to take into account some phenomena. Especially, we want to reduce overshoots, which are occurring at the start and at the end of turns. We want to anticipate curvatures changes.

Experiments[3] have been conducted on a flat grass field (Figure 16). The reference trajectory is a serpentine (Figure 15): a sequence of 30 m straight lines and turns with curvature radius of 4 m. On results graphs, curves are indicated by a grey area.

Predictive control has been evaluated at 2 m/s and 1.5 m/s. In Figures 17 and 18, we clearly see that without prediction (red curves) the robot understeer at the beginning of each turn, and oversteer at the end of each of them. Using feedforward approach (green curves), we are limiting this phenomenon. At 1.5m/s, prediction effect is not as impressive as at 2m/s. However, a light improvement is visible adding prediction to backstepping command.

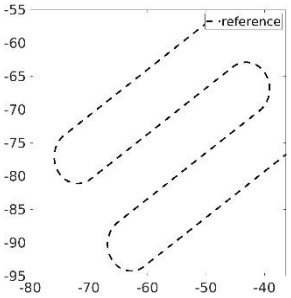

Figure 15. Serpentine

Figure 16. Experimental setup

[3] A video of the experimentis available at https://youtu.be/D3ltJFQA3_s

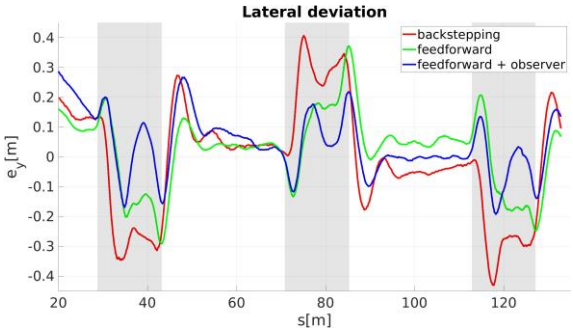

Figure 17. Impact of feedforward and observation at 2 m/s

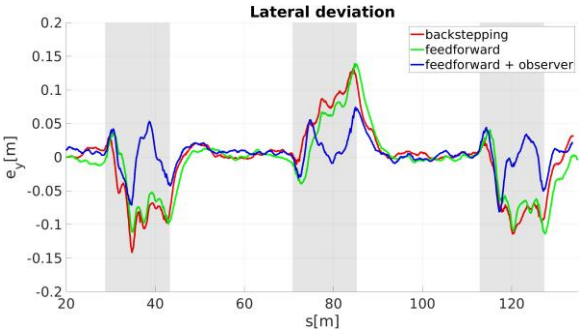

Figure 18. Impact of feedforward and observation at 1.5 m/s

Adding then adaptive control (blue curves), permits to have a better convergence during the steady-state of turns. In this experiment, we activate adaptive control only during turns. During straight line adaptive control is not necessary. Combining prediction and adaptation provides good performances at high speed.

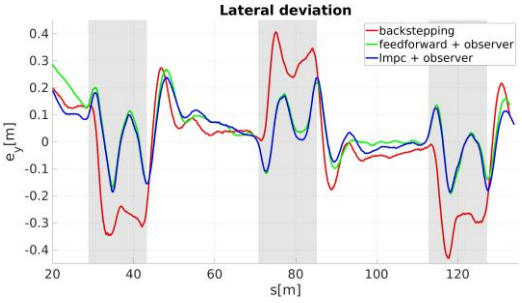

Figure 19. Comparison feedforward and LMPC at 2 m/s

Differences between feedforward and LMPC methods are not significant. At 1.5 m/s (Figure 20) LMPC is slightly better than feedforward. However, at 2 m/s (Figure 19) they seem to be equivalent. Nevertheless, both of them are providing really good results to follow a serpentine path.

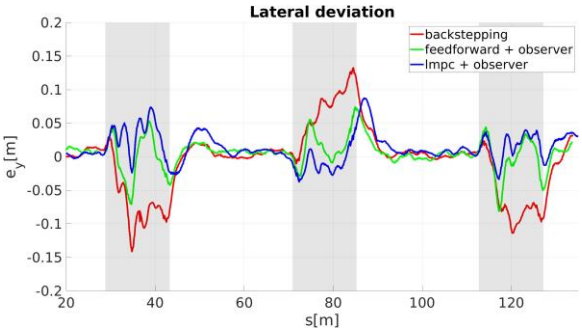

Figure 20. Comparison feedforward and LMPC at 1.5 m/s

V. CONCLUSION

In this paper, we presented two approaches to control longitudinal and angular speeds of robot. We then recalled kinematic models, observers, backstepping, adaptive control and predictive control.

These various strategies of path-tracking has been tried and tested in full-scale experiments with the crawler Ceol of Agreenculture. We highlighted the benefits of adaptive control to compensate model uncertainties, or when there are a lot of slipping phenomena, especially during curves at high speed on grass field or in hard slope. At straight line, slipping does not occur on Ceol thanks to its tracks. In that sense, we proposed to activate adaptive control only during turns. In order to estimate the sliding effects, different observers presented in the paper have been implemented, and their equivalence have been shown. In vineyard conditions, benefits of adaptive control has not been proved. In nominal work condition, backstepping control is sufficient to achieve the task of weeding with Ceol. Two predictive control methods have been presented. Both of them give similar results on a serpentine. Combining adaptive and predictive approach, we obtain really good performance of path-tracking, even at high speed.

The hard part of these experiments were gains tuning. For each speed change, or change of grip, gains had to be adapted. Further research will concern that aspect, trying to find optimal gains online, respecting real time constraints.

ACKNOWLEDGEMENTS

The author would thank Agreenculture and INRAE for making this work possible by allocating resources. This work is also supported by French National Research and Technology Agency (ANRT), under the grant CIFRE attributed to Agreenculture.

REFERENCES

Bouton N., Lenain R., Thuilot B., and Martinet P. (2007). *Backstepping observer dedicated to tire cornering stiffness estimation: application to an all terrain vehicle and a farm tractor*.

Dar T.M. and Longoria R.G. (2010). *Slip estimation for small-scale robotic tracked vehicles*.

Deremetz M. (2018). *Contribution à la modélisation et à la commande de robots mobiles autonomes et adaptables en milieux naturels*.

Fierro R. and Lewis F.L. (1997). *Control of a nonholomic mobile robot: Backstepping kinematics into dynamics*. Journal of Robotic Systems, 14.

González R., Fiacchini M., Guzmán J.L., Álamo T., and Rodríguez F. (2011). *Robust tube-based predictive control for mobile robots in off-road conditions*. Robotics and Autonomous Systems, 59.

Gu D. and Hu H. (2002). *Neural Predictive Control for a Car-like Mobile Robot*.

Kanjanawanishkul K., Hofmeister M., and Zell A. (2009). *Smooth Reference Tracking of a Mobile Robot using Nonlinear Model Predictive Control*.

Kokotovie P.V. (1992). *The Joy of Feedback: Nonlinear and Adaptive*.

Lenain R., Deremetz M., Braconnier J.-B., Thuilot B., and Rousseau V. (2017). *Robust sideslip angles observer for accurate off-road path tracking control*. Advanced Robotics, 31.

Lenain R., Thuilot B., Cariou C., and Martinet P. (2006). *High accuracy path tracking for vehicles in presence of sliding: Application to farm vehicle automatic guidance for agricultural tasks*. Autonomous Robots, 21.

Moosavian S. and Kalantari A. (2008). *Experimental slip estimation for exact kinematics modeling and control of a Tracked Mobile Robot*.

Morin P. and Samson C. (2008). *Motion control of wheeled mobile robots*.

Nagesh I. and Edwards C. (2013). *A Multivariable Super-Twisting Sliding Mode Approach*.

Picard G., Lenain R., Laneurit J., Thuilot B., and Cariou C. (2020). *A predictive control framework for edge following: Application to two types of mobile robots*.

Shi G., Yang J., Zhao X., Li Y., Zhao Y., and Li J. (2016). *A H-Infinity Control for Path Tracking with Fuzzy Hyperbolic Tangent Model*. Journal of Control Science and Engineering, 2016.

Tomis V., Martin M., Duparque A., and Boizard H. (2014). *Impact of deep compaction on root growth and yield of potato*.

Wang Z., Su C., Lee T., and Ge S. (2004). *Robust adaptive control of a wheeled mobile robot violating the pure nonholonomic constraint*. In (Vol. 2).

Wit J., Crane III, C.D., and Armstrong D. (2004). *Autonomous ground vehicle path tracking*. Journal of Robotic Systems, 21.

Xiao H., Li Z., Yang C., Zhang L., Yuan P., Ding L., and Wang T. (2017). *Robust Stabilization of a Wheeled Mobile Robot Using Model Predictive Control Based on Neurodynamics Optimization*. IEEE Transactions on Industrial Electronics, 64.

Measurement Data Recording and Preprocessing for Training Data Generation using ROS

Benjamin Kazenwadel*, Simon Becker, and Marcus Geimer

Institute of Mobile Machines (Mobima), Karlsruhe Institute of Technology (KIT), Germany

* Corresponding author: <benjamin.kazenwadel@kit.edu>

Abstract: The ongoing development of automated machine control systems amplifies the necessity of large-scale data acquisition and storage. Data collection and preprocessing have a major impact on the quality of the developed systems and therefore have to be optimized and monitored. Especially for machine learning systems preprocessing is a key factor to assure functionality. Our measurement setups are based on ROS and connect a variety of sensors and data sources to one network. The data collection was thereby automated with a variety of developed software tools that feature a simple graphical user interface for quality monitoring and reducing the effort for the operator during the data collection process.

In this paper, we present the developed data collection tools and the preprocessing tools to convert the data into training data for neural networks to help other researchers in their data collection tasks.

Keywords: ROS, CAN, Data Collection, Data Processing

I. INTRODUCTION

Vehicle internal data transfer relies on higher level communication protocols such as SAE J1939 or CANopen in order to regulate and control the data transmission (Geimer 2020; Truck Bus Control and Communications Network Committee 2020).

The definition and fixed structure of these protocols provide message collision protection due to a priority definition between the different control units, and error correction to identify and correct transmission failures (Pfeiffer et al. 2008).

On the primary level, these protocols use Controller Area Network (CAN) as a physical data transmission layer as defined in ISO 11898-1 and ISO 11898-2 to connect multiple electronic control units to a shared data transmission interface (ISO 11898-1:2015. *Road Vehicles – Controller Area Network (CAN).* Part 1: *Data Link Layer and Physical Signalling*, 2015; ISO 11898-2:2016. *Road Vehicles – Controller Area Network (CAN).* Part 2: *High-Speed Medium Access Unit*, 2016).

Due to the message arbitration process, two CAN participants which are on each end of the BUS must be able to communicate within the time frame of a message. This limits the usable length of the BUS with an increase in data rate (Pfeiffer et al. 2008).

The increase in necessary sensor technology in mobile machinery led to the development of more sophisticated CAN standards. These new standards include CAN-FD and ISOBUS.

The CAN-FD standard was developed using flexible data rates to increase communication bandwidth. (Hartwich 2012)

The ISOBUS (ISO 11783) standard establishes communication between the different electrical components in agricultural vehicles to simplify the connection process between any tractor and implement, independent of the manufacturer. The standard is based on J1939, but features additional transport protocols for high data volumes and navigation data (ISO 11783:2017. *Tractors and Machinery for Agriculture and Forestry – Serial Control and Communications Data Network*, 2017).

Table 1 gives an overview on the maximum transmission rates of some CAN-based communication standards.

Table 1. Maximum Transmission Rate of Communication Standards (Geimer 2020; Hartwich 2012)

Standard	Maximum Transmission Rate
SAE J1939	500 kbit/s
CANopen	1 Mbit/s
CAN-FD	15 Mbit/s

There is also the option to install multiple CAN networks in the same machine. This is sufficient for many use cases, since most of the connected devices only require a few other devices for their proper functionality, and therefore the information distribution can be separated into different networks (Geimer 2020).

In most machines, central Electronic Control Units (ECUs) have access to multiple CAN networks to establish communication in between, if necessary.

These advantages of using these CAN systems are useful for transmitting short numerical data, e.g., speed measurements or pressure levels, but come at the cost of limiting the flexibility of data types that can be transmitted through them.

Dedicated recording hardware can be used for data collection. These devices record all incoming CAN messages to be later analyzed using software such as CANoe, CANalyzer, CANape, and vSignalyzer (*CANlog – Data Logging with CANlog*, n.d.).

There is also the possibility for real-time data analysis, with a variety of different applicable hardware and software combinations. A comparison of a few of these real-time capable options can be found in (Rohrer et al. 2019).

These systems are limited to recording CAN data.

The advancement of sensor technology in the last years led to the requirement of adding camera systems and 3D-scanning technology to the machinery. Due to the bandwidth limitations of standard CAN bus protocols, difficulties arise in transmitting the requested data in an appropriate time interval.

The Ethernet standard provides additional network speed and thereby allows the transmission of large quantities of sensor data at high speeds, which is necessary for instance for the recording of point clouds measured by stereo camera systems.

Furthermore, Ethernet networks are cost-efficient and can be easily deployed since there is no necessity of specifying information priority and data structure in comparison to the CAN-bus protocols (Geimer 2020).

The usage of the robot operating system (ROS) as a communication standard in measurement and robotic setups simplifies the connection between sensors and programs in measurement setups, using Ethernet as the central communication protocol.

The free and open-source framework allows connecting a variety of different hosts and programs (nodes) to make their information accessible across the whole measurement setup. ROS drivers are available for a wide variety of sensor types and models. The information exchange is thereby supervised by a ROS master, a program that connects the different nodes if they require information from each other. The information can hereby range from numerical data and coordinate transformations to complex data types such as camera images or point clouds from laser scanners or stereo cameras. This enables easy installation and expandability during hardware changes, since the communication is not specifically adjusted to one use case.

Measurement data can be collected in files called rosbags, that record the incoming data streams from the different sources with their recording timestamp. These files can then be played back to develop control systems or visualize the recorded content (Quigley et al. 2009).

This framework streamlines tasks of connecting different sensors and provides the infrastructure for merging the sensor's respective data streams into a centralized data storage. The adaptable setup structure is especially important for monitoring and controlling heavy-duty tasks such as agricultural processes, since measurement setup changes occur frequently in these use cases.

These changes range from planned modifications, for instance during implement exchanges, to unscheduled sensor replacements, since most sensors are not rated for these harsh environments and therefore have to be exchangeable during the collection process.

A variety of additional open-source software is available to extend the functionality of ROS for data recording processes. In the following, we would like to give a brief introduction to the two most significant packages.

Plotjuggler is an independent tool to inspect and visualize rosbags and other measurement data files or data streams within an interactive graphical user interface. The tool feature plugins that allow for real-time tracking of ROS topics (Faconti 2016/2022).

The Rosbag Database is a web-based tool to maintain an overview of the collected rosbags. Their contents are scanned and entered into a database to easily search and identify relevant recordings for data analysis.

It can be mounted using the included docker image and features user authentication to limit access to the web interface (Southwest Research Institute (SwRI), 2016/2022).

For optimizing the machine control systems, communication in between the standard CAN-bus and additional sensors, which are connected via Ethernet using ROS, must be established. Currently, this can be achieved by dividing these information channels and logging CAN data independently using CAN-loggers, and simultaneously recording rosbags for the additional sensors.

The recorded data can then later merged for a holistic analysis. This approach is inefficient and leads to an additional workload. Furthermore problems such as synchronisation offsets can occure due to multiple unconnected timers.

In this paper, we propose a connection between the CAN-bus network and a ROS system on an Ethernet network to merge data streams and simplify data recording processes.

There has been a similar proposal to establish this connection in a car. However, the focus of this work lies on making internal signals available as lightweight as possible for integration on a Raspberry Pi (Elmadani et al. 2021).

To collect data from mobile working machines, the whole amount of different signals on the BUS has to be accessible in a simple manner whereas the computational power is available and system robustness a necessity.

II. CONNECTING CAN AND ROS

We developed a software bridge to connect the vehicle's internal CAN-Bus to the ROS system on the Ethernet network to establish mutual information exchange.

Using this bridge, CAN-data is accessible in the ROS network and all sensor data can be recorded simultaneously into a single rosbag.

These rosbags can then be analyzed and stored in a database as visualized in Figure 1.

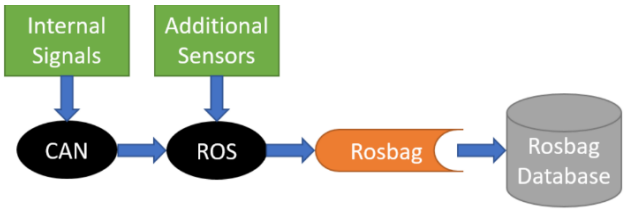

Figure 1. Collection Process

This approach allows for simplified holistic analysis and optimization of control systems and is especially important for the training of neural networks.

Furthermore, control nodes, that rely on receiving and transmitting information from both networks, can now be developed in ROS and do not require an individual hardware interface to the CAN (Figure 2).

These control systems can preprocess data to reduce the required rosbag storage space or directly interact with system components to perform work tasks.

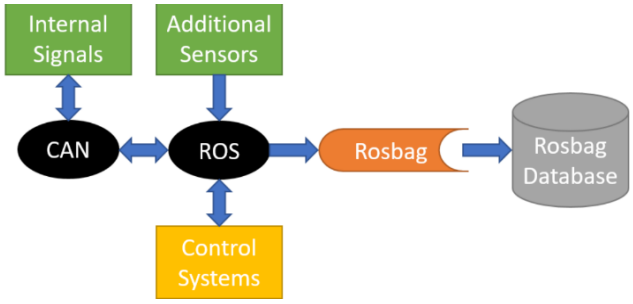

Figure 2. Control Process

In CAN-communications, information about the relevant messages is usually specified in .dbcfiles. These files contain the respective identifiers for each message, the relevant bytes in the received byte arrays, and further information for decoding the incoming data stream.

Furthermore, outgoing messages can be defined in these files to make them readable for other connected sensors and ECUs. Our software bridge accomplishes these tasks by automatically making all topics available that are specified in a .dbc file for reading and writing operations on the CAN. The ROS-node uses the openly available software package can-dbcparser (Auracher 2013/2013) to access the content of the specified .dbc files and then adds ROS subscribers and publishers (Datatype: std_msgs/Float32) for the specified CAN messages. Furthermore, there is the option to automatically send a custom ROS messages that contain a timestamp in addition to the numerical values. This automated functionality is crucial since it makes the adaption to new vehicles simple and fast.

III. SUPERVISING DATA COLLECTION

Due to the large quantity of sensor data exchanged in the ROS network, supervision of the data collection process is crucial. This involves automated collection tools, tagging of the recordings, as well as overall system supervision to detect sensor failures and system overload.

Our collection tools are plugins for Rqt.

Rqt is the standardized tool to visually display information in ROS. The plugin-based tool can be modified intuitively to the respective preferences. A variety of plugins are already included in the standard ROS installation for machine control as well as data visualization.

The plugins can be dragged and dropped to modify the interface for the respective use case.

A. Recording

Our measurement setups started with a simple CAN interface that was then made accessible to the ROS setup. Since additional sensors such as stereo cameras and laser scanners were added soon afterward, the usage of the command line to record all incoming messages into a single rosbag file was not feasible, and a topic selection was necessary due to the size of the incoming data stream.

The rqt-bag plugin, that comes with the standard full ROS installation, features the option to record only relevant topics.We realized that for a simple data recording, many of the included features are not required and an increase in performance would be more beneficial for the collection process. Therefore, the plugin was adapted to feature fewer options and increase recording reliability.

This adapted version resulted in the creation of the rqt-mobimabag plugin.

The plugin automatically names the recorded bags using the date and time. However, a custom name can be set and there is also the option for automated naming using the information published to the *metadata* topic.

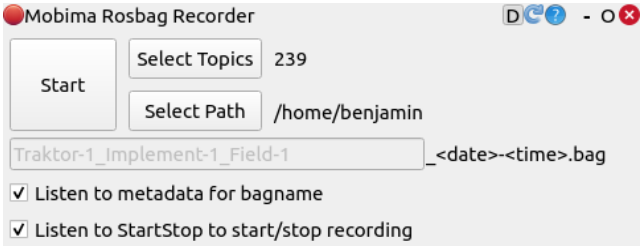

Figure 3. Recording Plugin

Since our operating processes often contain specified start and stop operations, such as when a driver presses a button to lower the implement at the beginning of a row and to raise it at the end, this information can be used to automate the collection process since the plugin can listen to a ROS topic to start and stop the collection process.

B. Additional Parameters

The rqt-userparameter plugin was developed to add a standardized way of including recording parameters into the rosbag files under the *\metadata* topic.

This topic is used by the rosbag database to add tags to the rosbags for a simplified overview of the collection settings.

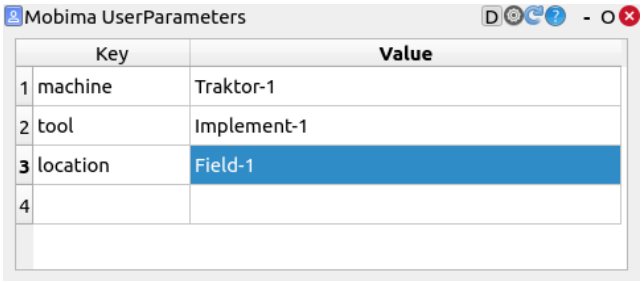

Figure 4. Userparameter Plugin

For our tasks, the relevant information was the type of machine, the implementat, and the location during the collection process. Further information can be added, such as weather conditions or driver information.

The first three selected parameters can also be combined with the rqt-mobimabag plugin to automatically name the rosbags during data recording.

C. Sensor Fault Detection

As our data collection is focussed on heavy-duty operations, sensor faults and connection issues are common problems. To detect these issues, we developed a lightweight tool that inspects the rate of incoming ROS messages and informs the user visually if a sensor is not sending data to the network. After a selection of the monitored topics, topics that receive messages within the specified time threshold are marked green, whereas the other topics are marked red and moved to the top of the list.

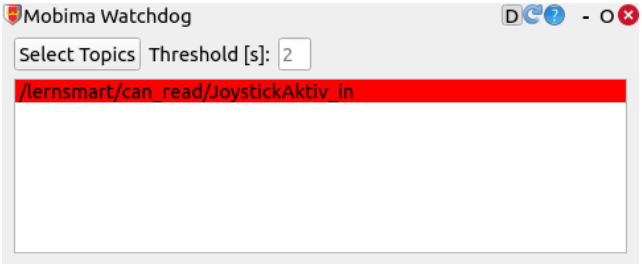

Figure 5. Sensor Supervision Plugin

IV. DATA PROCESSING

Rosbag recordings are similar to CAN-BUS recordings in a way that each piece of information is stored in a separate message.

Additionally, each recorded ROS message features information about the topic type as displayed in Table 2.

Table 2. Rosbag Message Format Example

Time [ns]	Topic	Type	Content
1637847573.5	/speed	std_msgs/Float32	data: 0.5
1637847573.6	/angle	std_msgs/Float32	data: 20.0
1637847574.5	/dist	std_msgs/Float32	data: 2.5
1637847574.6	/speed	std_msgs/Float32	data: 2.5

However, for the training of neural networks, a description of the overall system state is necessary since the commonly used software libraries such as TensorFlow and Keras are optimized to take whole system states at once as input data for supervised neural networks and reinforcement learning algorithms (Chollet et al. 2015; Martín Abadi et al. 2015).

To solve this issue, the separate incoming message streams must be merged into a combined system state information stream, as visualized in Table 3.

Table 3. Training Data Format Example

Time	Speed	Angle	Distance
1637847574.0	0.5	20.0	NaN
1637847575.0	2.5	20.0	2.5
…	…	…	…

Our training data extraction tool samples the rosbag records by a selectable frequency to combine the latest

measured values by each sensor at each of the sampling points.

The time information is thereby given by the rosbag timestamp, which is set during the data recording process.

The tool also allows searching for rosbags that contain the required topics and checks their message frequencies to identify faulty recordings where sensor data is missing.

After that, each topic can be filtered using a running average or a running median filter, to be then merged with the other specified topics in the next step. This is especially useful if the measurement data is noisy and includes various sensor frequencies, since the filtering step relies on a fixed time interval and therefore includes all recorded messages rather than being limited to the sampling frequency.

The sampled data is then saved in easily applicable .csv files, which are compatible with commonly used neural network libraries.

The tool can only be applied to data topics and not on images or point clouds.

The idea behind the tool is based on a script by Nick Speal (Speal 2014/2014) and expanded to merge the information from different topics into a single file using the rosbag python API. In comparison to other rosbag to .csv conversion tools, this approach allows for the extraction of data of all currently installed ROS-message types instead of being limited to the standard message types or a list of hard-coded message types.

The tool requires having ROS installed and is then able to extract information from standard messages and all custom message types that are installed on the system.

All software tools can be downloaded from: https://git.scc.kit.edu/mobima/publications/datarecording

V. EVALUATION

Time delays need to be avoided during data collection to provide an accurate representation of the recorded process. This is crucial for the further development of controlling algorithms, since their design needs to be optimized on measurement data to reduce the effort of practical testing.

Since many computational steps are involved during our measurement data collection in ROS, an analysis of the time delay caused by the software bridge between CAN and ROS and by the rosbag recording tool is necessary.

The evaluation was conducted on a Lenovo P14s Notebook which played back CAN recordings from the Forwarder.

This machine resembles one of the use-cases for the software presented in this paper (Geiger et al. 2021).

Other use-cases include new control systems for agricultural machinery as in (Becker et al. 2022).

One CAN signal was selected and monitored to identify time offsets until the saving into the rosbag file. Therefore, the timestamps were recorded on receiving the CAN messages, at the time the associated ROS-message was created in the CAN-Bridge, and the specified rosbag recording time. Figure 6 visualizes the delay of the respective time in comparison to the timestamp of the CAN-message reception.

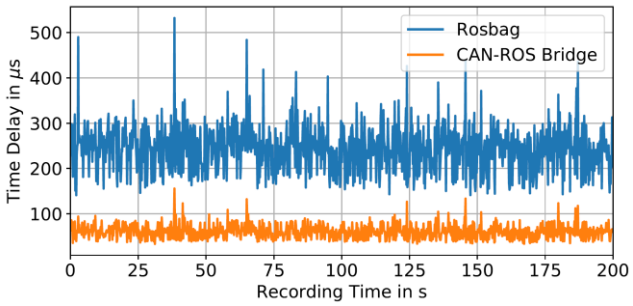

Figure 6. Recording Time Delay

The numerical offsets are stated in Table 4.

These offsets show that very fast-acting control systems should use the time stamp set by the CAN bridge to avoid timing offsets and fluctuations associated with further data transmission and subsequent storage in the rosbags.

However, the use of the rosbag time stamp is sufficient for a status description of the overall system as described in the data processing section since the deviations are comparatively small compared to the time interval between two signals on the CAN assuming standard transmission frequencies in mobile machines.

Table 4. Time Delays

Measurement Location	Average Delay in microseconds	Maximum Delay in microseconds
CAN-ROS-Bridge	60	243
rosbag	156	532

Further research has to be conducted on the limitations of the proposed measurement system. This includes recording speed capabilities, and overall system reaction time, to identify the limitations for the usage in high-speed control systems.

VI. CONCLUSION

This paper describes an exemplary setup for large-scale data collection using ROS. It describes the individual tools required for recording, monitoring, and expanding the measurement setup to include CAN signals as new data sources. We hope that we can help other scientists in their research by making our recording tools available to the public. Furthermore, we hope that the ROS community can provide support for the further development of these tools.

We're currently planning the transition to ROS2, therefore, our packages will be adapted to the new standard in the future for more real-time applicability. (Maruyama et al. 2016)

REFERENCES

Auracher M. (2013). *Can-dbcparser* [C++]. https://github.com/downtimes/can-dbcparser (Original work published 2013).

Becker S., Kazenwadel B., and Geimer M. (2022). *Automation and Optimization of Working Speed and Depth in Agricultural Soil Tillage with a Model Predictive Control based on Machine Learning*, LAND.TECHNIK 2022 The Forum for Agricultural Engineering Innovations, 55–64; https://publikationen.bibliothek.kit.edu/1000143315

CANlog – Data Logging with CANlog (n.d.). Vector Informatik GmbH. Retrieved April 18, 2022; https://www.vector.com/int/en/products/products-a-z/hardware/canlog/

Elmadani S., Nice M., Bunting M., Sprinkle J., and Bhadani R. (2021). *From CAN to ROS: A Monitoring and Data Recording Bridge*. Proceedings of the Workshop on Data-Driven and Intelligent Cyber-Physical Systems, 17–21. https://doi.org/10.1145/3459609.3460531

Faconti D. (2022). *PlotJuggler 3.4* [C++]. https://github.com/facontidavide/PlotJuggler (Original work published 2016).

Geiger C., Beiser S., and Geimer M. (2021). *Automated Driving on a Skid Road with a Forwarder in a CTL Logging Process*. Proceedings of The Joint 43rd Annual Meeting of Council on Forest Engineering (COFE) & the 53rd International Symposium on Forest Mechanization (FORMEC), Forest Engineering Family – Growing Forward Together, September 27–30, 2021, Corvallis, Oregon, U.S.A., W. Chung (Ed.), 135; https://publikationen. bibliothek.kit.edu/1000139443

Geimer M. (2020). *Mobile working machines*. SAE International; https://doi.org/10.4271/9780768094329

Hartwich F. (2012). *CAN with flexible data-rate*, CAN Newsletter, 2/2012, 10.

ISO 11783:2017. *Tractors and Machinery for Agriculture and Forestry – Serial Control and Communications Data Network. (2017)*. International Organization for Standardization; https://www.iso.org

ISO 11898-1:2015. *Road Vehicles – Controller Area Network (CAN).* Part 1: *Data link layer and physical signalling* (2015). International Organization for Standardization; https://www.iso.org

ISO 11898-2:2016. *Road vehicles – Controller area network (CAN).* Part 2: *High-speed medium access unit*. (2016). International Organization for Standardization; https://www.iso.org

Maruyama Y., Kato S., and Azumi T. (2016). *Exploring the performance of ROS2*. Proceedings of the 13th International Conference on Embedded Software, 1–10; https://doi.org/10.1145/2968478.2968502

Pfeiffer O., Ayre A., and Keydel C. (2008). *Embedded networking with CAN and CANopen: Requirements for understanding embedded networking code and communications, the underlying CAN technology, selecting CAN controllers, implementation options, application-specific examples of popular device profiles* (Rev. 1. Ed.). Copperhill Technologies Corp.

Quigley M., Conley K., Gerkey B., Faust J., Foote T., Leibs J., Wheeler R., and Ng A. (2009). *ROS: An open-source Robot Operating System*, 3.

Rohrer R.A., Pitla S.K., and Luck J.D. (2019). *Tractor CAN bus interface tools and application development for real-time data analysis*. Computers and Electronics in Agriculture, 163, 104847; https://doi.org/10.1016/j.compag.2019.06.002

Southwest Research Institute (SwRI) (2022). *Bag Database* [Java]. Southwest Research Institute Robotics; https://github.com/swri-robotics/bag-database (Original work published 2016).

Speal N. (2014). *ROStools* [Python]; https://github.com/nickspeal/ROStools (Original work published 2014).

Truck Bus Control and Communications Network Committee. (2020). *SAE J1939 Functional Safety Communications Protocol*. SAE International; https://doi.org/10.4271/J1939-76_202004

Development of a Loading Assistance System for Wheel Loaders

J. Lommatsch*, A. Ulrich*

Technische Hochschule Köln, Betzdorfer Str. 2, 50679 Cologne, Germany

* Corresponding authors: joerg.lommatsch@th-koeln.de, alfred.ulrich@th-koeln.de

Abstract: A joint research project at the TH Köln together with Pfreundt GmbH is investigating networked optimization of work processes, using wheel loaders as the model machine. The optimization is expected to result in a considerable increase in efficiency (e.g., efficiency rate, fuel efficiency). A new generation of intelligent and autonomous loading processes, with the purpose of significantly assisting users and reducing work load, will be created for mobile work machines using methods of artificial intelligence.

In the past years a steady increase in digitalization of business processes and automation of systems could be observed. This trend is clearly visible in research and development goals within mobile work machines sector. This research project will take into consideration the interface between human and machine during automated loading operations, applying artificial intelligence to achieve an overall improvement in control and safety functions.

Keywords: Wheel Loader, Assistant System, Energy Efficiency, Productivity, Loading Process Automatization

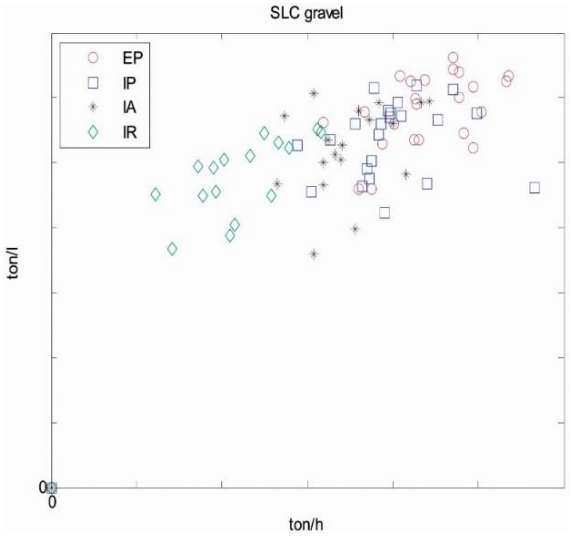

Figure 1. The fuel efficiency and productivity in SLC gravel [FRA12]

I. INTRODUCTION

The wheel loader is a versatile work machine used for a variety of loading and transport tasks in different applications (e.g., mining, bulk material industry, demolition and recycling, etc.). Vehicle fuel consumption has been a focus of manufacturers even before the constant presence of climate change discussions.

Frank [FRA12] investigated the differences between operator types in four varying levels of experience (inexperienced, average, trainer/test driver, professional). Results showed that the fuel efficiency had a positive correlation to the level of experience of the driver. The differences lay at up to 200% in fuel consumption and up to 700% in the handling capacity. The most important conclusion of the study is that a noticeable reduction in the power consumption of the entire work cycle can best be achieved by reducing the power consumption during the loading phase of the shovel. Although this work phase represents only a maximum of 25% of the total cycle time, it is responsible for up to 40% of the fuel consumption. Similar results were attained by Baumgarten [BAU14] during an investigation of the loading process of a tractor with attached front loader.

Through consequent application of machine learning to the loading process of a wheel loader, in addition to the interface between human and machine, the current project will significantly improve the complete work process of a mobile work machine with the following targets:

- **Process Optimization:** Increase economic efficiency by up to 50% higher handling/loading efficiency, even in sub-optimal working conditions, such as weather conditions, difficult to load earths and differences in operator experience.
- **Energy Efficiency:** Minimization of energy consumptions (e.g., fuel consumptions).
- **Resource Saving:** Service life optimized machine operations – up to 40% reduction in wear at the shovel through use of the floating position and wear-optimized loading processes; predictive maintenance.
- **Safety:** Operator alleviation during monotonous work and/or work that poses a hazard to health through autonomous work functions.

The increase of up to 50% in handling efficiency will be achieved through a networked, model-supported measurement and control system of the drive and the hydraulic dumping and lifting system of the wheel loader, where a sensor will capture, analyze and trans-

mit the loading process as actual value for the networked control loop. A software tool, operating in parallel for machine learning of the loading process, will independently execute an optimized loading process, in line with the methods of artificial intelligence, as soon as sufficient parameters and functional correlations have been collected.

By using the methods of artificial intelligence, a new generation of intelligent and autonomous productions systems in mobile work machines will be generated, which will support and alleviate people in their daily work.

The first step towards a fully automated wheel loader will be consideration of the work portions with the largest impact on energy efficiency and performance, which have the greatest optimization potential. Even if the uptake of bulk material represents 25% of the loading process, it is responsible for up to 40% of the fuel consumption. Additionally, this work portion has a huge importance to the determination of productivity.

II. MARKET SITUATION

The increase in performance of imbedded systems (processors, memory, sensors, actuators, etc.), the high degree of networking and the omnipresent availability of data and services makes it possible to create increasingly autonomous systems, which can aggregate all-encompassing environmental data and react versatilely and independently to its working environment [BET13].

Especially in the automotive industry, assistance systems that support safety and process efficiency are already widespread. The autonomously driven cars from Tesla, Inc. are one such example.

In contrast to this, corresponding systems have not found application very often in the construction industry, despite the steady increase in market demand.

Several loading systems are already available on the market.

- Cat Payload (Caterpillar, Inc.)

The Cat Payload-System, made by Caterpillar, Inc., is a weighing system in series production, which assists the operator during off-loading of the bucket. Data delivered by angle sensors and the hydraulics of the boom cylinders are used for payload calculation. The system is designed to assist in reaching the daily payload goals [CAT22].

- AutoDig (Caterpillar, Inc.)

The AutoDig is a loading system, which makes automatic loading of the bucket possible. The main focus lies in the increase of productivity. This means that the system is designed for attaining the maximum loading capacity of the wheel loader [CAT22].

- Tip Off Assist (Caterpillar, Inc.)

The Top Off Assist weights the bucket load and sums up the nominal content of each bucket load until an operator determined total weight has been achieved. The system automatically tips to remove excess material in the last bucket load so that the specified total weight is achieved. This prevents over-loading of dump trucks [CAT22].

- Auto Set Tires (Caterpillar, Inc.)

The Auto Set Tires System assists the operator during the loading process by optimizing the bucket load such that greater pressure is put on the front tires, resulting in higher traction with the underground. This significantly decreases skidding of the tires. This is implemented by a light lifting command during loading. This eliminates the greater portion of tire skid [CAT22].

- Truck Payload Assist (Liebherr S.A.)

The Truck Payload Assist has a very similar functionality to the Tip Off Assist from Caterpillar, Inc. The driver enters the desired total load weight and the system suggests an optimal target weight for the individual bucket fillings, as well as the number of loading cycles necessary for a uniform loading operation [LIE22].

- Load Assist (Volvo Group AB)

The Load Assist has functionality identical to the Tip Off Assist by Caterpillar Inc. The driver enters the desired total load weight, the system weights the bucket loading and sums up the nominal content of each bucket up until the target weight. At the touch of a button, the system automatically tips the bucket to remove material until the desired total weight is reached in the last bucket filling [VOL22].

The systems described give a rough idea of the assistance systems currently available on the market. This clearly shows that the steady increase in demand for efficiency presents a necessity for new solutions.

III. RESEARCH PROJECT “LADE-RAD”

A wheel loader is a mobile work machine used to transport payload over short distances. Wheel loaders

are mainly used in earth moving, mining and road construction applications and, next to hydraulic excavators, they form an important market segment in the area of construction and working machines. These machines work in cycles. This means that their operation and movement patterns are consecutive and have very few concurrent process steps. The work cycle of a wheel loader is divided into the driving and loading cycles.

The typical driving cycle of a wheel loader is a Y-driving cycle. If seen from above, the typical driving movements form a Y-shape.

Figure 2. Y-driving cycle of a wheel loader [GUS22]

The loading process can be split into four subprocesses:

1 – driving to the loading area,
2 – loading bulk material,
3 – transport to delivery area,
4 – unloading bulk material.

Since subprocess 2 – loading bulk material – has the greatest impact on energy efficiency and performance, this process will be isolated within this research project. Especially the theories offered by Pieczonka and Dudzinski [PIE96] have been taken into consideration in developing of the optimal loading strategy for different bulk goods and soils because their studies show that

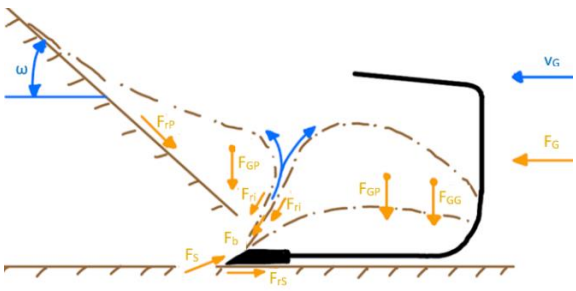

Figure 3. Level model for a digging operation [according to KUN11]

a dynamically stimulated loading bucket can have a positive effect in energy efficient loading. The dynamic excitation during the loading process helps overcome the flow limit of the bulk material and aids in settling the material, which increases the bulk material density and allows more material to be loaded.

A temporary and needs-based dynamic excitation of the loading bucket has a positive influence on the velocity of the bucket movement and, therefore, also the digging force FG. However, with increasing speed, negative influences also appear, such as a rise in deformation resistance and soil strength. This process can still have a positive effect, especially with medium to difficult loading soils, since the bucket is usually loaded in layers. The method of dynamically exciting the bucket and related consequences for the loading process and on the bulk material/soil is a point studied in the research project by KLB/TH Köln.

In order to isolate this effect and the loading process itself, a test stand was developed with which such dedicated investigations are made possible.

The test stand is based on the multi-functional Avant 218, which is available at the research institute and with which laboratory tests can later be verified.

Figure 4. CAD Model Wheel Loader Test Rig [GUS22]

The entire kinematics (green) and even the loading shovel are from a real Avant 218. The test stand was modelled with help of the simulation software available in Matlab Simulink.

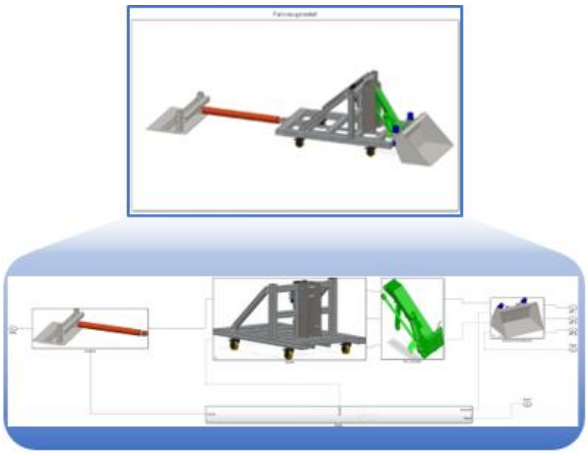

Figure 5. Vehicle model with subsystems [GUS22]

During initial tests of the simulation, a bucket tip movement path that had been previously manually recorded was used as the basis for the motion simulation. Both trajectories run practically along an identical path, but in the simulated line (blue), an exact analysis shows that there are slight deviations from the recorded path trajectory. This minimal deviation can be explained by play in the bucket, which is also considered in the simulation.

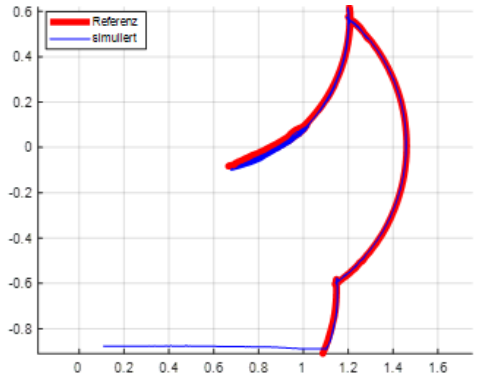

Figure 6. Comparison of path trajectories: real (red) and simulated (blue) [GUS22]

First attempts with the test stand model and the vibration motors were able to give an initial assessment of the effect of the motors on the loading result. A sand-gravel mixture with particle size of 0/16 was used in this investigation. The experiment runs were:

1 – without activation of the vibration motors,
2 – activation of the vibration motors at 40% power,
3 – activation of the vibration motors at 80% power,

The results showed that activation of the vibration motors at 40% power offered no noticeable improvement in the bulk material loading, while activation of the motors at 80% power showed an increase in bulk material loading of approximately 9%. An increase of the vibration motor power to 100% a further increase can be expected.

IV.CONCLUSION

First investigations with the final construction stage of the demonstrator test stand already show a very good approach. As a result of the selected bulk material mixture, it is not always possible for the vibration motors to adequately cause the material to flow and support loading of the bucket sufficiently. Further experiment runs will be completed to determine the optimal frequency, amplitude and vibration level for the type of bulk material. Investigations with different bulk materials and difficult to load materials are also planned. Especially in the latter, supporting the loading process with vibration motors could allow direct loading of the material with the wheel loader bucket, rather than having to use other tools or machines to loosen material prior to loading.

New insights from these experiments serve as a basis for self-learning loading assistance systems for wheel loaders.

REFERENCES

[BET13] Bettenhausen K.D. und Kowalewski S., *Thesen und Handlungsfelder Cyber-Physical Systems: Chancen und Nutzen aus Sicht der Automation*, Düsseldorf: VDI, 2013.

[CAT22] Caterpillar, Inc., “Caterpillar”, retrieved January, 2022; http://www.cat.com

[FRA12] Frank B., Skogh L., Filla R., Fröberg A., Alaküla M., *On increasing fuel efficiency by operator assistant systems in a wheel loader*, In: Tagung VTI 2021, Changchun (China).

[GUS22] Gusmao Vickus M., *Multi-body simulation of a wheel loader test bench for the investigation of dynamic loading processes*. Masther Thesis, Technische Hochschule, Köln 2022.

[KUN11] Kunze G., Mieth S., Voigt S., *Bedienereinfluss auf Leistungyzklen mobile Arbeitsmaschinen*, ATZ offhighway, Sonderausgabe ATZ (April 2011), S. 70–79.

[KUN12] Kunze G., Göhring H. und Klaus J., *Baumaschinen – Erdbau- und Tagebaumaschinen*, Wiesbaden: Vieweg+Teubner Verlag, 2012.

[LIE22] Liebherr S.A, “Liebherr”, retrieved January, 2022; http://www.liebherr.com

[PIE96] Pieczonka K., Dudzinski P., *Bucket Loader Research in Technical University of Wroclaw*. 1st International Conference on Off-Road Machines and Vehicles in Theory and Practice, 23.–24. September 1996, Wroclaw, Poland.

[VOL22] Volvo Group AB, “Volvo Group”, retrieved January, 2022; https://www.volvoce.com

CIDEA: Robot behavior adaptation from interactive communication with buried sensor nodes. Application to smart agriculture

Laure Moiroux-Arvis*, Christophe Cariou, François Pinet, and Jean-Pierre Chanet

[1] University of Clermont Auvergne, INRAE, UR TSCF, 9 av. Blaise Pascal CS 20085, F-63178 Aubière, France

* Corresponding author: <laure.moiroux-arvis@inrae.fr>

Abstract: The combination of the recent advances in Wireless Underground Sensor Networks (WUSNs) and mobile robotics enable today to consider the development of more efficient and accurate systems. In particular, the measurement to the ground conditions from a set of sensor nodes buried at a few dozens of centimeters deep and distributed in a farm field would enable to adapt the behavior of some agricultural robots accordingly. To that end, this paper presents the development of a buried sensor node operating in LoRa with a collector node embedded on a mobile robot. When the robot is close to the sensor node, the soil moisture measurement is taken into account by the collector node to adapt the speed of the robot accordingly. The experimental results reported in this paper demonstrate the capabilities of the proposed system.

Keywords: Wireless Underground Sensor Networks, Soil moisture, Mobile robotics, LoRa, Agriculture

I. INTRODUCTION

In recent years, the development of mobile robotics has increased significantly in agriculture, whether it be to increase farm productivity, perform environmentally friendly operations or relieve human operators from tedious and unhealthy work (Oliveira et al. 2021). Many challenges remain, however, to be faced to obtain fully operational robots. One of them is to provide for the robot the capacity to take into account the ground conditions in the field to adapt its behavior accordingly. In particular, when the soil moisture varies significantly, the speed of the robot and the tuning of its agricultural tool have to be adapted, see the illustration in Figure 1.

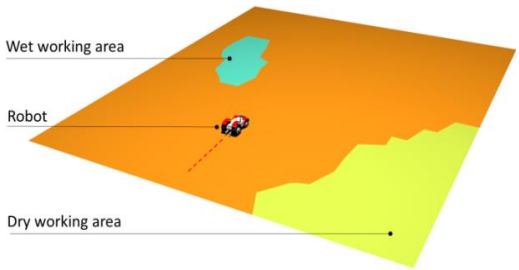

Figure 1. Variability of the soil moisture in a field requiring to adapt the working speed of the robot and its tool accordingly

Nevertheless, the access to the information of soil moisture, locally and in real time, is a real issue. Microclimate weather stations and connected devices can be positioned at the edge of the field, but they are not sufficient to obtain local and accurate information of the soil moisture within the areas (Tenzin et al. 2017). In addition, such systems can obviously not be positioned and multiplied inside the field as they represent obstacles for the farming activities.

The recent advances in Wireless Underground Sensor Networks (WUSNs) and Internet of Underground Things (IoUT) have however opened new opportunities. These approaches are based on the development of sensor nodes able to operate underground at a few dozens of centimeters deep; see Figure 2 and (Moiroux-Arvis et al. 2022; Saeed et al. 2019; Salam et al. 2020). Different measurements can be carried out, as the soil moisture and temperature. The data are emitted by the radio modules, also buried underground, using Low-Power Wide Area Networks (LPWAN) as LoRa technology (Augustin et al. 2016). A device located aboveground, e.g., a gateway or a data collector embedded on an Unmanned Aerial Vehicle (UAV), can communicate with the buried sensor nodes and retrieve the measurements, see (Cariou et al. 2022; Popescu et al. 2020).

Figure 2. Buried sensor node measuring the moisture of the soil and emitting the data through radio communication

The advantage to bury and dissimulate all the components underground, including the radio modules and the antennas, is to protect the system against potential damages due to farming activities but also adverse weather conditions, animals, theft and vandalism. The main current applications of WUSNs are smart irrigation, landslide detection, and monitoring of underground infrastructure, see (Akyildiz et al. 2006; Ferreira et al. 2019; Silva et al. 2010).

The development of buried sensor nodes is, however, a challenging task as the electromagnetic radio waves are highly attenuated in the soil, about 20–300 times worse than in the air (Da Silva et al. 2014). This attenuation is, moreover, dependent on numerous environmental factors (e.g., volumetric water content (VMC), burial depth, soil composition). The communication ranges are therefore considerably reduced and highly variable. In practice, the Underground to Underground (UG2UG) communication link between two buried sensor nodes is limited to a few meters. However, as highlighted in our last work (Moiroux-Arvis et al. 2022), the Underground to Aboveground (UG2AG) communication link can reach more than 250 meters under certain conditions, i.e., 868-MHz radio modules with LoRa communication, transmit power of +14 dBm/25 mW and a burial depth about 15 cm.

Based on these first results, the objective of this paper is to demonstrate that a data collector node embedded on a mobile robot is able, in real time, to retrieve the soil moisture of a buried sensor node when passing at proximity and adapt the working speed of the robot accordingly. This is the objective of the project named "CIDEA" which is funded by the CAP 20-25 International Research Centre – Innovative Transportation and Production Systems (CIR-ITPS). The principle scheme is presented in Figure 3.

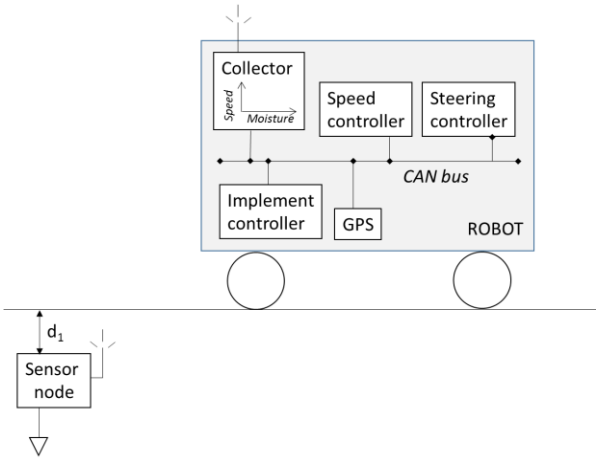

Figure 3. The robot adapts its working speed with respect to the soil moisture information collected from a buried sensor node

This paper is organized as follows. Sections II, III and IV present, respectively, the methodology, the experimental design and the experimental results. Sections V and VI present the conclusion and the discussion.

II. METHODOLOGY

The methodology consists first to bury underground a sensor node at a depth d_1 below the surface, see Figure 3. This sensor node regularly measures the soil moisture and emits a data frame using its LoRa radio module.

A collector node is embedded on the mobile robot and connected to its CAN bus. It has reading access to various information on the CAN bus (e.g., GPS position, status of the implement, robot's speed) and can write a CAN message to change the speed of the robot if required.

When the robot is inside the coverage range of the buried sensor node (a_1 in Figure 4), the collector node receives and decodes the data frames which contain the soil moisture information. It will take the control of the speed of the robot with respect to the RSSI (Received Signal Strength Indication) signal level: if the strength of the RSSI signal is above a threshold (–65 dBm), the soil moisture information is taken into account and the speed of the robot is adapted according to the curve presented in Figure 5. When the robot leaves the delock area (–80 dBm), the collector node gives back the control of the speed to the controller of the robot.

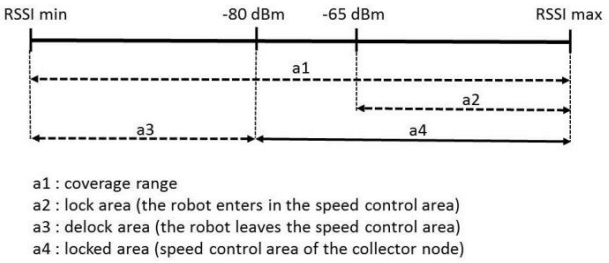

Figure 4. Speed control area of the collector node

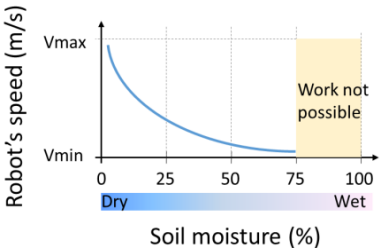

Figure 5. Speed of the robot with respect to soil moisture

III. EXPERIMENTAL DESIGN

A. The buried sensor node

We developed a buried sensor node based on a microcontroller Atmega328-AU 8 MHz (Microchip) and a LoRa radio module RFM95W (HopeRF) operating at 868 MHz, see Figure 6 and (Cariou et al. 2022) for more details.

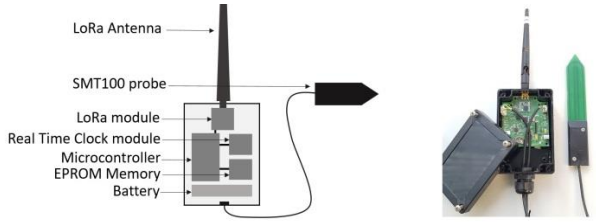

Figure 6. The buried sensor node

A Truebner SMT100 probe is connected to measure the soil moisture. The sensor node is powered with a rechargeable lithium battery 3.7 V/8.8 Ah. A temporal reference DS1378 is implemented to switch between the deep-sleep and active modes. The node is activated during the measurement of soil moisture (the measurements are stored on a 8 bit memory EEPROM with I2C-bus interface) and during predetermined time-windows to communicate the data from the radio module. When a time-window is active, the sensor node puts its radio module in listening mode and waits for a message from the collector node. When the communication is established, the sensor node transfers the data to the collector node.

B. The collector node

The collector node is built around a microcontroller Atmega328-AU (Microchip) running at 8 MHz, see Figure 7. It is powered through a rechargeable lithium battery 3.7 V/8.8 Ah. It is equipped with a LoRa radio module RFM95W (HopeRF) to communicate with the buried sensor node, and a CAN bus interface to exchange information with the robot (read and write access). All the data of the experiments are stored in a SD card in the collector node enabling to analyze the results afterwards.

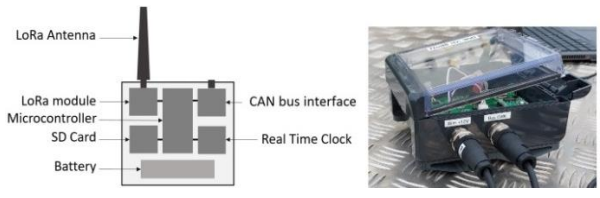

Figure 7. The collector node on the robot

The sequence of operations and decisions made by the collector node is presented in Figure 8. The collector node scans on the RF communication (LoRa radio module) the proximity of a sensor node. When a sensor node is detected, the quality of the radio signal is measured (RSSI signal) to determine the speed control area. Every second, an interruption routine reads different data on the CAN bus (e.g., GPS position, actual speed of the robot) and stores them on the SD card.

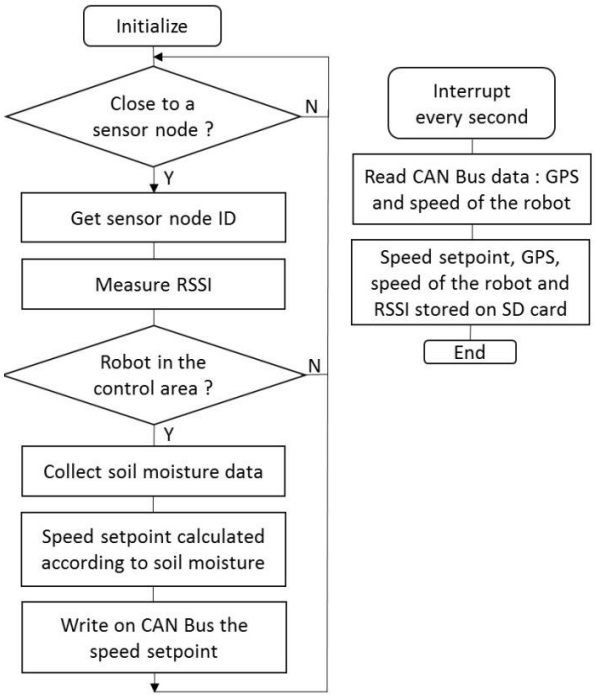

Figure 8. Diagram of the program in the collector node

C. The mobile robot

The mobile robot used for the tests is presented in Figure 9. This robot is electrically propelled (Lithium-ion batteries 12.8 kWh). The wheelbase is 1.40 m for a total length of 2.50 m. The track is adjustable from 0.70 m to 1.30 m. It weights about 550 kg with a maximal payload of 150 kg. It has four independent wheeled-motors and four independent steering actuators. It is able to reach speeds up to 10 m/s in the wide track configuration. The implement at the rear is a horizontal sprayer. Four nozzles are placed at different working distances, they can be activated independently.

The architecture of this robot is built around three main controllers (steering, speed, implement) joined by two CAN bus. The collector node is connected to the CAN bus enabling to take the control of the speed of the robot.

Figure 9. Experimental robot used for the tests

IV. RESULTS

A. The experimental setup

The sensor node is buried at the depth d_1 = 15 cm. Four soil moistures were tested: 0%, 5%, 10% and 20%. At the beginning of each experiment, the robot is manually controlled with its joystick (speed and steering). When the collector node detects the buried sensor node with a RSSI value higher than –65 dBm (i.e., very good reception, that enables to limit the size of the experimental area), it controls the speed of the robot in place of the joystick (from 0 to 1 m/s, see Figure 10). When the RSSI signal becomes lower than –80 dBm, the collector node gives back the control of the speed to the joystick.

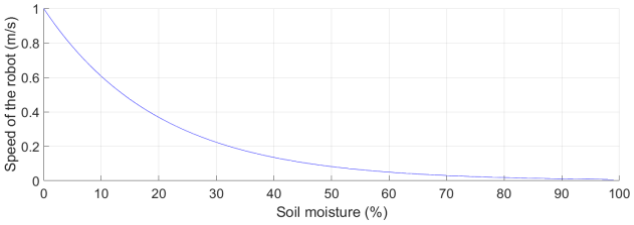

Figure 10. Speed of the robot with respect to the soil moisture

B. Results with 0% soil moisture

For the first experiment, the probe is not connected leading to a measured soil moisture of 0%. According to Figure 10, that leads to a setpoint for the speed of 1 m/s. Figure 11 presents the trajectory of the robot and Figure 12 the RSSI level measured by the collector node. The time during which the collector node controls the speed of the robot is depicted in red. The speeds of the robot (setpoints and measurement) are presented in Figure 13.

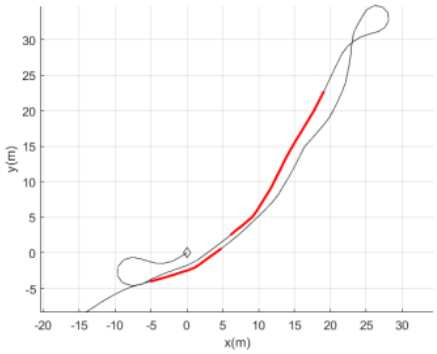

Figure 11. Trajectory of the robot – Test 0%

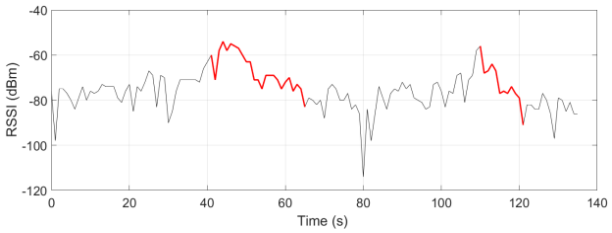

Figure 12. RSSI received by the collector node – Test 0%

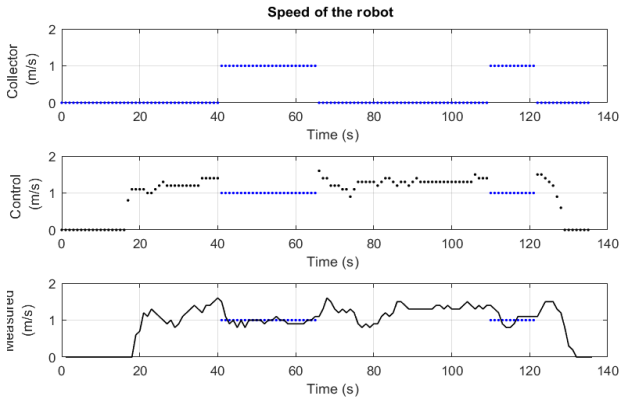

Figure 13. Speed controls and measurements – Test 0%. Up: speed calculation by the collector node (0 if not active), Middle: speed control from the joystick (black) and the collector node when active (blue), Down: measured speed of the robot

At the beginning (t = 0 s), the buried sensor node is detected but with a RSSI value equals to –80 dBm (i.e., not taken into account), see Figure 12. The robot is then moved and controlled with the joystick. At t = 40 s, the RSSI signal becomes upper than –65 dBm. The robot is then controlled by the collector node until the time t = 65 s (i.e., the RSSI value becomes lower than –80 dBm). This is also the case between t = 110 s and t = 122 s. On the top of Figure 13, we clearly observe the commands of the collector node (v = 1 m/s), the commands of the speed of the robot from the joystick and the collector node (middle of Figure 13), and the effective speed of the robot (bottom of Figure 13).

C. Results with 5%, 10% and 20% soil moisture

The probe is then connected to the buried sensor node. Successively, three experiments are carried out with a dry soil (5% humidity), a slightly wet soil (10% humidity) and a wet soil (20% humidity). The results are presented in the Figures hereafter. For the three experiments, it can be clearly observed that when the buried sensor node is detected with a RSSI value higher than -65 dBm, the collector controls the speed of the robot.

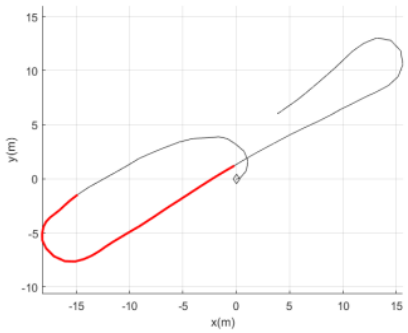

Figure 14. Trajectory of the robot – Test 5%

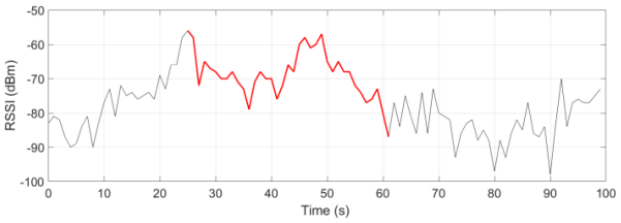

Figure 15. RSSI received by the collector node – Test 5%

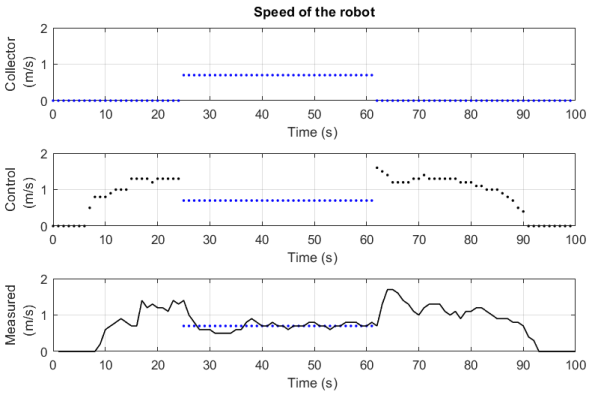

Figure 16. Speed controls and measurements – Test 5%

In Figure 16, it can be observed for example that the speed of the robot was about 1.5 m/s at the beginning of the experiment. When the robot enters in the speed control area with the buried sensor node, its speed is constrained to be reduced at 0.7 m/s. In Figure 19, the speed is reduced to 0.5 m/s, and to 0.3 m/s in Figure 22.

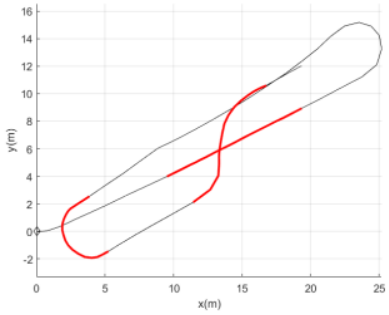

Figure 17. Trajectory of the robot – Test 10%

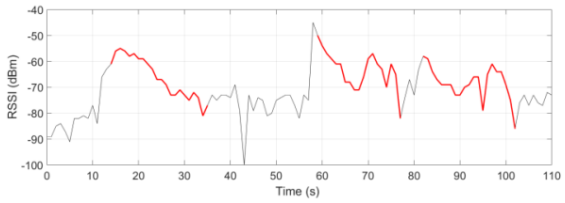

Figure 18. RSSI received by the collector node – Test 10%

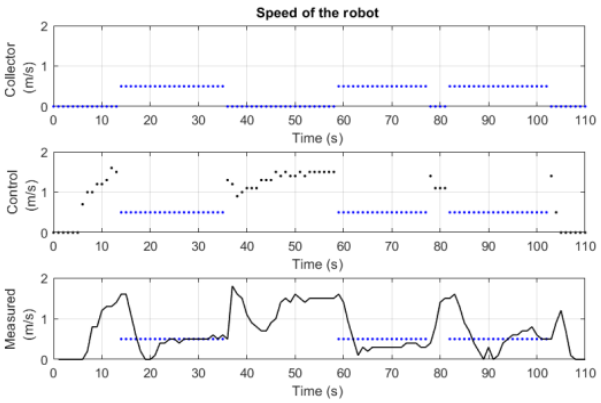

Figure 19. Speed controls and measurements – Test 10%

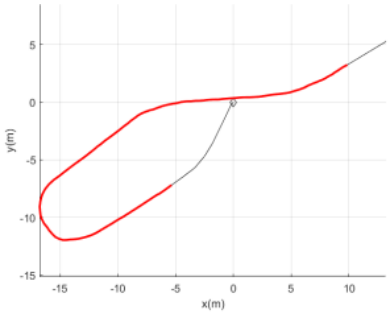

Figure 20. Trajectory of the robot – Test 20%

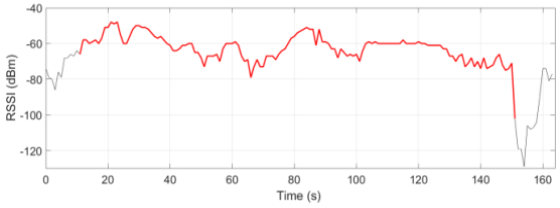

Figure 21. RSSI received by the collector node – Test 20%

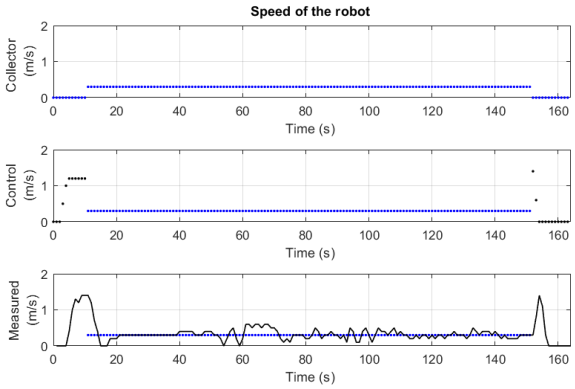

Figure 22. Speed controls and measurements – Test 20%

V. CONCLUSION

The objective of this paper was to demonstrate the possibility to adapt the behavior of a mobile robot to the variations of the soil moisture encountered in a field. To access information on soil status as close as possible to the intervention area of the mobile robot, we proposed to develop a system based on sensor nodes buried at a few dozens of centimeters deep. The main challenge is however to develop these underground objects with relevant communication ranges. Constraints on energy consumption and transmit power also have to be considered as the nodes have to work ideally several years without battery replacement.

We developed a set of buried sensor nodes able to measure the soil moisture and transmit that information to an aboveground collector node. The radio communication is based on the technology LoRa at 868-MHz. The collector node is embedded in a mobile robot and connected to its bus CAN. It has read and write access, in particular to control the speed of the robot when required. The first experimental results are presented. When the robot is in the communication range of a buried sensor node with a RSSI value upper than a threshold, the moisture information is collected and used to adapt the speed of the robot accordingly.

VI. DISCUSSION

The first results obtained in this paper have considered a single sensor node located underground. In the future work, we intend to study several sensor nodes positioned in a field. That requires to carefully study and manage the overlapping areas. In particular from the knowledge of the position of the robot and the locations of the different moisture sensors in the field, the setpoint for the robot's speed could be determined with precision. Obviously, the speed curve with respect to the soil moisture could also be adapted to the situation. The exponential shape of Figure 8 was only used to rapidly reduce the speed of the robot with respect to the soil moisture. A more in-depth study on the evolution of the speed of the robot according to the humidity of the soil could be carried out.

Moreover, the system can take advantage of the circulation of the mobile robot in the field to collect the soil moisture data. These measurements are local and accurate, and are particularly useful to improve the management of the crops (e.g., irrigation planning, spatial distribution of the water).

FUNDING

The work presented in this paper is part of the project called "CIDEA". This research is financed by the French government IDEX-ISITE initiative 16-IDEX-0001 (CAP 20-25) – Innovative Transportation and Production Systems (CIR-ITPS). It aims to demonstrate a proof-of-concept applied to an agricultural context. The opportunity to bury and dissimulate a panel of sensors underground also opens new perspectives in other activity sectors.

REFERENCES

Akyildiz I.F., Stuntebeck E.P. (2006). *Wireless underground sensor networks: Research challenges*, Ad Hoc Networks, 4, 669–686, DOI: 10.1016/j.adhoc.2006.04.003.

Augustin A., Yi J., Clausen T., Townsley W.M. (2016). *A study of LoRa: long range & low power networks for the Internet of Things*, Sensors, 16, 1466, DOI: 10.3390/s16091466.

Cariou C., Moiroux-Arvis L., Pinet F., Chanet J.P. (2022). *Data collection from buried sensor nodes by means of an Unmanned aerial vehicle*, Sensors, 22, 5926, DOI 10.3390/s22155926.

Da Silva A.R., Moghaddam M., Liu M. (2014). *The future of wireless underground sensing networks considering physical layer aspects*, The Art of Wireless Sensor Networks, 2, 451–484, DOI: 10.1007/978-3-642-40066-7_12.

Ferreira C.B.M., Peixoto V.F., de Brito J.A.G., de Monteiro A.F.A., de Assis L.S., Henriques F.R. (2019). *UnderApp: a system for remote monitoring of landslides based on wireless underground sensor networks*, WTIC, Rio de Janeiro, Brasil.

Moiroux-Arvis L., Cariou C., Chanet J.P. (2022). *Evaluation of LoRa technology in 433-MHz and 868-MHz for underground to aboveground data transmission*, Computers and Electronics in Agriculture, DOI: 10.1016/j.compag.2022.106770.

Tenzin S., Siyang S., Pobkrut T., Kerdcharoen (2017). *Low cost weather station for climate-smart agriculture*. 9th Int. Conf. on Knowledge and Smart Technollogy, DOI 10.1109/KST.2017.7886085.

Oliveira L.F.P., Moreira A.P., Silva M.F. (2021). *Advances in agricultural robotics: a state-of-the-art review and challenges ahead*, Robotics, 10, 52, DOI 10.3390/robotics10020052.

Popescu D., Stoican F., Stamatescu G., Ichim L., Dragana C. (2020). *Advanced UAV–WSN System for Intelligent Monitoring in Precision Agriculture*, Sensors, 817, DOI: 10.3390/s20030817.

Saeed N., Alouini M.S., Al-Naffouri T. (2019). *Towards the Internet of Underground Things: a systematic survey*, IEEE Communications Surveys Tutoials, 21 (4), 3443–3466, DOI: 10.1109/COMST.2019.2934365.

Salam A., Raza U. (2020). *Current advances in Internet of Underground Things*, Signals in the Soil, 10, 321–356, DOI: 10.1007/978-3-030-50861-610.

Silva A.R., Vuran M.C. (2010). *(CPS)2 Integration of center pivot systems with wireless underground sensor networks for autonomous precision agriculture*. IEEE/ACM International conference on Cyber-Physical Systems, Stockholm, Sweden, DOI: 10.1145/1795194.1795206.

Methods for developing an assistance system for slip control of a wheeled paver

Marius Nono Tamo, Prof. Alfred Ulrich

TH Köln, Betzdorfer Straße 2, 51103 Cologne, Germany

Corresponding author: Marius Nono Tamo; <marius.nono@th-koeln.de>

***Abstract*:** The aim of this work is to develop an assistance system to reduce the slip occurring on the drive wheels of a paver, with regard to quality assurance of the road surface during the paving process. For example, the developed system can improve the longitudinal evenness of the road paved by the wheeled paver by using a tractive force management system. The methods to realise this assistance system is presented here.

Keywords: Wheeled pavers, Asphalt roads, Building quality, Slip control, Traction effort, Dislocation resistance

I. MOTIVATION

Various road construction machines are used to build asphalt roads (Figure 1). Dump trucks deliver the hot paving material from the mixing plant to the construction site. The material is transferred either directly to the paver or via a feeder, which supplies the paver with the paving material via a conveyor belt without direct contact between the two machines. The paver builds the pre-compacted asphalt road using the screed at a preset paving height, profile and width as well as tamper stroke, speed and vibration frequency. Final compaction of the paved asphalt road surface takes place with the road rollers (Kappel, 2016).

Figure 1. Road construction process
with the road construction machines involved

According to the type of track unit, road pavers are divided into tracked and wheeled pavers. Tracked pavers have crawler tracks and thus achieve higher traction. They are therefore more powerful and suitable for paving roads with greater widths. Wheeled pavers, on the other hand, have two large rear wheels and two to four smaller front steering wheels. Compared to tracked pavers, wheeled pavers can reach higher travel speeds and thus offer easier transport and relocation options. Furthermore, a wheeled paver with independent suspension is better able to negotiate obstacles such as manhole covers, in that each wheel individually compensates the difference in height over the manhole cover in turn due to the independent suspension. In contrast, a tracked chassis is rigid and lifts up as a result of the lack of suspension, which in turn affects the entire paver (Kappel 2016). In this work, only wheeled pavers are considered, as the slip that occurs with these is much greater than with tracked pavers.

II. ASSIGMENT OF TASKS

To ensure the acceptance of the paved road after completion of the construction process, the specifications set by the client, such as pavement thickness, width, transverse profile, longitudinal evenness and degree of compaction, must be met. Many factors must be considered when completing the road to be paved and meeting the specified requirements. If the required parameters are not met after completion, deviations in the specified construction quality can occur, which in turn can lead to considerable costs due to reworking. The guarantee of a good paving quality of the road depends upon, among other things, a qualitatively good condition of the paving material as well as a flawless functionality of the road construction machines used and their interaction. During the paving process, the paving screed of the road paver is lowered onto the paving material and pulled over it in the direction of paving so that the asphalt solidifies. During this process, the paving screed floats on the paving material. For the production process of the asphalt layer, it is therefore indispensable that the paver moves evenly along the planned road on the pre-treated base so that the high demands on the quality of the road can be ensured. This requires sufficient traction of the drive tyres (Ulrich 1996).

According to the German standard DIN18317, the required evenness for each layer is defined within a 4 m long measuring distance as followed:

- For the asphalt layer ≤1 cm;
- For the asphalt binder layer ≤1.5 cm;
- For the asphalt base layer ≤2 cm.

The aim of this work is to develop an assistance system for slip control for a road paver with a wheeled undercarriage. This is to be used to automatically control and thus minimise the slip that occurs during the paving process within a defined target range. For this purpose, the existing tractive force or the displacement resistance of the paving material in front of the screed is continuously determined with sensors. The assistance system being developed will use the measured variables to derive and display a tractive force balance on the paver, to better identify the cause of slippage. To identify the cause of slip, special attention will be paid to the proportion of the dislocation resistance exerted by the paving material in front of the paving screed. It is to be determined what effect the filling level of the mix in the auger chamber and the material properties have on the slip. The existing slip is to be determined by comparing the target and actual speeds. In view of the fact that a certain slip is always present, the actual slip determined is to be compared with a specified target slip in the control loop of the control system to be worked out. If a deviation is detected between the target slip and the actual slip and the causes are determined, the tractive force will be automatically adjusted by the slip control system through anticipatory adjustment of the material.

III. METHODS AND RESULTS

The development work here is divided into various steps that are done in a fixed sequence. First, various variables influencing the tractive force of the wheeled paver were analytically investigated. Then, within the framework of the experimental investigations on the mobile working machine or on a test bench, the relevant influencing variables were recorded with suitable sensors. Using the results from the previous work steps, a simulation model was created that simulated both the machine behaviour and the interaction between the working machine and the paving material or the environment. This model will be used in a later work step to test the mathematically determined controller for the control of functionality before this is done in the real machine.

A. Analytical investigation of the influencing variables

Figure 2 shows the general force balance on a wheeled paver during the paving process. When paving with a feeder, there is no resistance to the movement of the truck R_{Truck} during the feeding process. The paver travels behind the feeder without contact.

The forward movement of the paver depends on the horizontal force components. However, some are influenced by certain vertical force components. For example, the adhesion force T_{Drive} depends on both the weight of the tractor and the weight of the material $F_{W,Mat}$ in the hopper. This means that a decrease or an increase of the amount of material in the hopper will affect adhesion traction. The same applies to the truck's resistance movement. For the sake of simplicity, the influence of the truck's resistance to movement is not taken into account here.

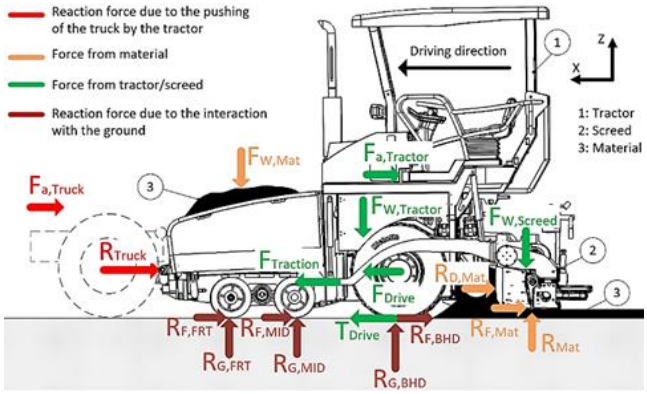

Legend: RTruck: Movement resistance of the truck; **Fa,Truck:** Acceleration force of the truck; **FW,Mat:** Weight force of the material; **RD,Mat:** Dislocation resistance of the material; **RD,Mat:** Friction force between screed and material; R**Mat:** Material's reaction force due to the screed's weight; **Fa,Tractor:** Acceleration force of the tractor; **FW,Tractor:** Weight force of Tractor; **FW,Screed:** Weight force of the screed; **FTraction:** Tractor's traction effort for screed's movement; **FDrive:** drive force from Motor; **TDrive:** transmitted tractive effort on the ground; **RF,FRT/MID/BHD:** Tyre's rolling resistance at the front/middle/behind; **RG,FRT/MID/BHD:** Wheel load at the front/middle/behind

Figure 2. Representation of the forces acting on the paver during the paving process on a horizontal road

The horizontal force components are subdivided into drive forces or tractive effort, working and driving resistances. The drive forces are the forces provided by the left or right travel drive for the forward movement of the construction machine. Tractive efforts are the tractive forces transmitted by the driven tyres on the road surface, which are generated due to the frictional connection between the two. The working resistance is the driving resistance exerted by the paving material. This is made up of the dislocation resistance and the frictional force between the screed and the material. The movement resistance comprises the rolling friction on the paver's tyres and the movement resistance of the truck.

B. Experimental investigation
of the influencing variables

The use of appropriate measurement technology is required to record the various influencing variables. The measurement technology is part of the control system for slip reduction that is being developed. The various methods to measure the influencing variables are described below.

To determine the dislocation resistance $R_{D,Mat}$ of the paving material acting in front of the screed, the traction effort $F_{Traction}$ is measured at the traction point of the left and right side of the tractor at the pull arms of the screed. The horizontally aligned traction effort is made up of the equally horizontally aligned dislocation resistance and the horizontal component of the frictional force $R_{F\text{-}Mat}$ between the paving screed (the screed plates) and the road surface (Figure 2). The frictional force $R_{F,Mat}$ is always inclined by the angle of attack β of the screed. It is the product of the screed weight $F_{W,Screed}$ (or the portion of the screed weight acting normally on the screed plate/paving material contact surface) and the coefficient of friction. In practice, the coefficient of friction $\mu_{R,B}$ between the screed plate and the asphalt material is in the range of 0.25–0.35 (PAST, 2012). By subtracting the friction force from the resulting tensile force (the sum of the measured tensile forces at the left and right tensile points), the dislocation resistance is obtained.

In order to measure the traction effort at the pull arms on the left and right side of the tractor, force measuring bolts were installed at the traction points (Figure 3). The force measuring bolt (FMB) was installed in such a way that it is loaded in the loading direction specified by the manufacturer. An anti-twist device prevents the FMB from twisting during use. The anti-rotation device is made by means of a form-locking connection between a plate screwed to the levelling rod and a groove provided on the FMB.

Figure 3. Illustration of the force measuring bolt installed at the traction point of the pull arm for recording the traction force

To record the existing slip S, two measured variables are of importance. This is the theoretical speed V_c and the (absolute) pave speed V_a. The slip can be determined by using the following formula:

$$S = \frac{V_c - V_a}{V_{Soll}} \times 100. \quad (1)$$

The theoretical speed corresponds to the circumferential speed of the driven wheel (here the rear wheel). It depends on the rotational speed n and the dynamic rolling radius r_{dyn}. In order to measure the rotational speed, a rotatory encoder was mounted at the rear wheel (Figure 4).

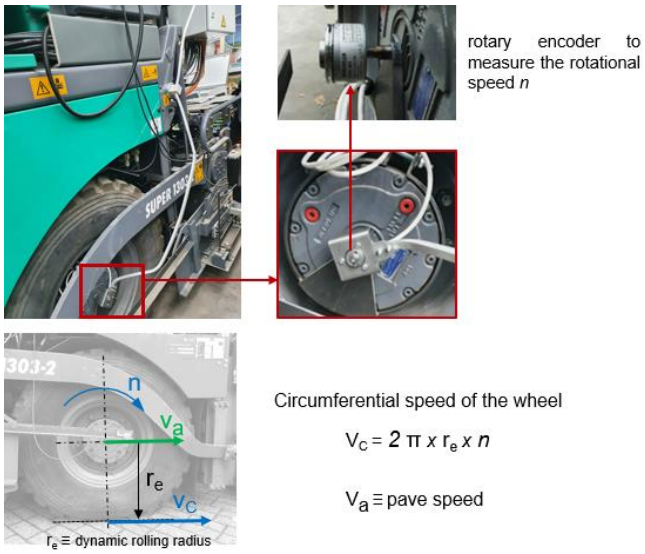

Figure 4. Measurement device for recording the rotational speed of the rear wheel and illustration of the dynamic rolling radius

During paving process, the pave speed is in the range of 2 to 6 m/min, which means that recording the (absolute) pave speed is a significant challenge. Below are some examples of sensors for low speed recording:

– Measuring wheel: this device has a very good accuracy and it can measure slow speeds. But slip can occur by using this sensor. Furthermore, obstacles such as stones can falsify the measurement.
– Global Positioning System (GPS) / Global Navigation Satellite System (GNSS): this measurement unit allows measuring drive speeds from 3.3 m/min on (VBOX). The disadvantage of the use of this device is the danger of signal loss due to the shadowing, which can affect the system.
– Cross-correlation measurement: can allow measurement of asbsolute speed less or equal 1.7 m/min.
– Kistler (2018). For this reason, this measurement device is more appropriate for task and was selected.

IV. CONTROL STRATEGY

The drive and slip control modules to be developed are shown in Figure 5 in the form of a cascade control.

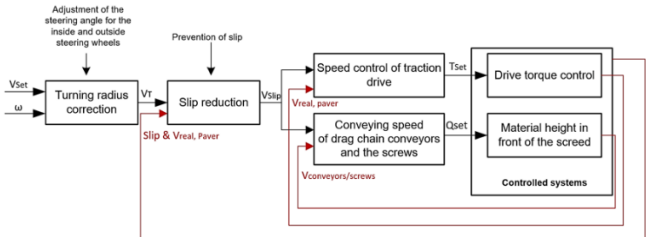

Legend: V_{Set}: Set point value for the speed of the paver; **ω:** Set point value for the turning radius; **V_T:** Longitudinal speed during cornering; **V_{Slip}:** Longitudinal speed after slip reduction; **T_{Set}:** Set point value for the drive torque; **Q_{Set}:** Set point value for the material flow in in front of the screed; **$V_{real,Paver}$:** real longitudinal speed of the paver; **$V_{conveyors/screws}$:** speed of the conveyors/screws

Figure 5. Traction and slip control modules in cascaded configuration

These comprise:

– A turning radius correction, which adjusts the setpoint of the steering angle for the outside and inside wheels.
– A slip reduction, which reduces slippage and enables optimum tractive force transmission with high frictional engagement.
– A speed control of traction drive, which guarantees a good transition behaviour in case of guiding and disturbance excitation and regulates the error quickly and accurately in a stationary manner. Strong overshooting of the controller or fluctuations in speed during operation must be avoided at all costs with regard to the installation process.
– A drive torque control receives the setpoint from the speed control and intervenes in the torque balance at the driven wheel (rear wheel). This is done by adjusting the voltage and pulsing the motor current directly in the power electronics.
– A control of material height in front of the screed, which regulates the quantity of paving material in front of the paving screed by controlling the conveyor speed as well as the screw speed.

V. OUTLOOK

In the next step, the experimental determination of the parameters as well as the design of the control system will be completed. Afterward, the developed control system will be tested in the simulation environment and then in the real machines.

REFERENCES

Kappel M. (2016), *Angewandter Straßenbau*, Springer Vieweg, Wiesbaden, p. 30.

Ulrich A. (1996), *Neue Straßenbautechnik*, TIEFBAU 11/1196, Heft 11, 108. Jahrgang, S.722–730, Erich Schmidt Verlag, München.

Vögele J. (2020), https://www.wirtgen-group.com/binary/full/o19402v89_SUPER_13003i_EN_StageV_2869493_mPW_0820.pdf [Last access: 10.2021].

Vögele J. (2020), https://www.wirtgen-group.com/binary/full/o19399v89_SUPER_13033i_EN_StageV_2869499_mPW_0820.pdf [Last access: 10.2021].

Research Project PAST (2012), *Prozesssicherer automatisierter Straßenbau*, Funding endicator: 19S8003C: duration of the project: 01.08.2008-31.07.2012

Steinmetzger R. (2003). *Bauproduktionstechnik – Grundlage der Maschinentechnik. Lehrunterlagen für Vertiefungsrichtung Baubetrieb*, Bauhaus-Universität Weimar, Weimar.

VBOX, https://www.vboxautomotive.co.uk/index.php/en/how-does-it-work-gps-accuracy [Last access: 11/2022].

Kistler (2018); https://www.kistler.com/files/download/960-252d.pdf?callee=frontend, p. 10 [Last access: 11/22].

WUST Publishing House prints
can be obtained via mailorder:
zamawianie.ksiazek@pwr.edu.pl
www.ksiegarnia.pwr.edu.pl

ISBN 978-83-7493-234-9
https://doi.org/10.37190/MCG2022